gene encoding the cholesterol side-chain cleavage enzyme, an essential enzyme for steroidogenesis) was integrated into the MSCs, and GFP-positive MSCs were then separated by fluorocytometry. Finally, to achieve the efficient differentiation of the isolated MSCs *in vitro*, the orphan nuclear receptor, steroidogenic factor (SF)-1 was ectopically expressed in MSCs. MSCs successfully differentiated into steroidogenic cells using any of these procedures. These results indicate that MSCs represent a useful source of stem cells for producing steroidogenic cells that may provide basis for their use in cell and gene therapy.

Materials and Methods

Animals

GFP transgenic rats [SD TgN(act-EGFP)OsbCZ-004] were kindly provided by Dr. M. Okabe (Osaka University, Osaka, Japan). Sprague Dawley rats were purchased from Sankyo (Shizuoka, Japan). At all times, the animals were treated according to National Institutes of Health guidelines. The donor animals used in this study were generally 4–5 wk old, and the recipient animals were 3 wk old.

Histology and immunofluorescence analysis

Immunohisto- and cytochemical staining with antirat P450 side-chain cleaving enzyme (P450scc) (C-16; Santa Cruz Biotechnology, Santa Cruz, CA), antimouse 3β-hydroxysteroid dehydrogenase I (3β-HSD I) (kindly provided by Dr. A. Payne, Stanford University Medical Center, Stanford, CA), antipig cytochrome P450 17 α-hydroxylase (P450c17) (kindly provide by Dr. D. Hales, University of Illinois at Chicago, Chicago, IL) or anti-GFP (Medical & Biological Laboratories Co., Ltd.) were performed on 10-μm frozen sections or cultured cells on glass slides using standard protocols. Appropriate Cy3- or fluorescein isothiocyanate-conjugated secondary antibodies (Sigma, St. Louis, MO) were used for detection.

Cell culture, stable transfection, and hormone assay

MSCs from GFP transgenic rats were collected and cultured as described by Pochampally *et al.* (14). Mouse (KUM9) (15) or human (hMSC-hTERT-E6/E7) (16) bone marrow-derived MSCs were maintained in Iscova's MEM or DMEM with 10% fetal calf serum. Plasmid DNA was transfected using the LipofectAmine PLUS reagent (Invitrogen, Carlsbad, CA) or calcium phosphate coprecipitation. Cells were used for the experiments after 10–12 passages, and steroid hormone production was sustained for at least 4 months. The levels of each steroid hormone in the media were measured by RIA.

Transplantation

Bone marrow cells from TgN(ActbEGFP) transgenic rats (1×10^6) were injected into the testes of 3-wk-old SD rats. Two to three weeks after transplantation, testes were removed to examine histochemically survival and differentiation of transplanted cells.

Plasmid construction

A 2.3-kb fragment of the human CYP11A (P450scc gene) promoter that functions specifically in steroidogenic organs (17) was obtained by PCR using pSCC2300-LacZ (kindly provided by Dr. B. C. Chung, Institute of Molecular Biology, Taipei, Taiwan) as a template and integrated into a promoter-less pEGFP-1 vector (CLONTECH, Palo Alto, CA). The *Eco*RI-*Stu*I restriction fragment, containing the CYP11A promoter-GFP, was then excised and inserted into *Eco*RI and *Swa*I site of pPUR (CLONTECH). The expression vector for rat SF-1 cDNA containing the entire coding region was generated by RT-PCR and subcloned into pIRES-puro2 vector (CLONTECH).

FACS analysis and cell purification

Cells were harvested by treatment with 0.25% trypsin/EDTA, after which they were neutralized with DMEM with 10% fetal calf serum, washed twice with PBS, and filtered through a 35-mm pore size nylon screen. FACS analysis was performed on a flow cytometer with a 488-nm argon laser and GFP-positive cells were isolated.

RT-PCR and real-time PCR

Total RNA from the cultured cells was extracted using the Trizol reagent (Invitrogen). RT-PCR was performed as described previously (18). The reaction mixture was subjected to electrophoresis in a 1.5% agarose gel, and the resulting bands were visualized by staining with ethidium bromide. Real-time PCR was performed as described by Rutledge and Cote (19). Reagents for real-time PCR were purchased from Applied Biosystems (Warrington, UK), except for SYBER green PCR master mix (QIAGEN, Valencia, CA). Reactions were carried out and fluorescence was detected on a GeneAmp 7700 system (Applied Biosystems). The primers used are shown in Table 1.

Western blot analysis

The extraction of protein from the cultured cells and subsequent quantification was performed as described previously (20). Equal amounts of protein (50 μg) were resolved by 12.5% SDS-PAGE and transferred to polyvinylidene difluoride membranes. Western blot analyses of SF-1, steroidogenic acute regulatory protein (StAR), P450scc, 3β-HSD I, P450c17, and β-tubulin were carried out with antisera directed against SF-1 (Ad4BP, kindly provided by Dr. K. Morohashi, National Institute of Basic Biology, Okazaki, Japan), StAR (kindly provided by Dr. W. Miller, University of California, San Francisco, CA) (21), P450scc (kindly provided by Dr. B. C. Chung) (22), 3β-HSD I (kindly provided by Dr. A. Payne), P450c17 (kindly provided by Dr. D. Hales) (23), and β-tubulin (D-10, Santa Cruz). ECL Western blot reagents (Amersham Pharmacia Biotech, Piscataway, NJ) were used for detection.

Results

Transplantation of rat bone marrow mesenchymal stem cells

In the prepubertal testis, fetal-type Leydig cells are replaced by adult-type Leydig cells, which originate from mesenchymal precursor cells that are present in the testicular interstitium (12). To determine whether MSCs can be engrafted into the testis and converted into steroidogenic cells we took 1×10^6 bone marrow cells from TgN(ActbEGFP) transgenic rats that had been maintained in culture (Fig. 1A) and injected them into the testes of 3-wk-old SD rats. As shown in Fig. 1C, donor engraftment was confirmed (100%) at various periods after transplantation (1–4 wk). A histochemical examination revealed that the GFP-positive cells present in the testes were located in the interstitium and were not observed within the seminiferous tubules (Fig. 1D). An immunohistochemical study showed that most of the GFP-positive cells in the interstitium were also positive for three Leydig cell markers, P450scc (Fig. 1E), 3β-HSD I, and P450c17 (data not shown). These results indicate that donor derived-plastic adhered marrow cells had in fact differentiated into steroidogenic Leydig-like cells *in vivo*.

Gene promoter sorting

Although these data suggest that the injected stem cells differentiated into Leydig cells, the apparent stem cell plasticity may also be explained by possible cell-nuclear fusion between donor and recipient cells, as has been recently suggested (24). Therefore, we next performed *in vitro* experiments to determine whether purified murine MSCs (mMSCs), KUM9 (15), have the capacity to differentiate into steroidogenic cells. To detect a cell population committed to

TABLE 1. Primers for RT-PCR and real-time PCR

Gene	Sequence	Gene	Sequence
RT-PCR		RT-PCR	
SF-1	F-CGCACAGTCCAGAACAACAAGCA R-CGGTTAGAGAAGGCAGGATAGAG	hHSD3b2	F-CAGTGTGCCAGTCTTCATCT R-AGCAGGAAGCCAATCCAGTA
mStAR	F-GAAGGAAAGCCAGCAGGAGAACG R-CTCTGATGACACCACTCTGCTCC	hP450c17	F-CATGCTGGACACACTGATGC R-GGTTGTATCTCTAAAATCTGT
mP450scc	F-TTCCGCTTTTCCTTTGAGTCCAT R-GTGTCTCCTTGATGCTGGCTTTC	hHSD17b3	F-GCAGATTTTACAAAAGATGACAT R-TCATGGGCAAGGCAGCCACAGGT
mHSD3b1	F-ACTGCAGGAGGTCAGAGCT R-GCCAGTAACACAGAATACC	hP450c21	F-TGCCTGCCTATTACAAATGT R-GGTGAAGCAAAAAAACCACG
mHSD3b6	F-TCTGGAGGAGATCAGGGTC R-GCCCGTACAACCGAGAATATT	hP45011 b1	F-ACATTGGTGCGCGTGTTCCTC R-GAGACGTGATTAGTTGATGGC
mP450c17	F-AAATAATAACACTGGGGAAGGC R-TGGGTGTGGGTGTAATGAGATGG	hP450 11b2	F-TACAGGTTTTCCTCTACTCG R-AGATGCAAGACTAGTTAATC
mP450c21	F-AGAGGATCCGCTTGGGGCTGC R-GGAGGAATTCCTTATGGATGGC	hP450aro	F-CTGGAAGAATGTATGGACTT R-GATCATTTCCAGCATGTTTT
mP450 11b1	F-TCACCAAATGTATCAAGAATGTGT R-CCATCTGCACATCCTCTTTCTCTT	β-Actin	F-GGGAAATCGTGCGTGACATTAAG R-TGTGTTGGCGTACAGGTCTTTG
mP450 11b2	F-CCAACAGATGTATCTGGAAGGTGC R-CCATCTGCACATCCTCTTGCCTCA	hIGF-2	F-AGTCGATGCTGGTGCTTCTACCTCTT R-TGCGGCAGTTTTGCTCACTTCCGATT
mLHR	F-CTCCACCTATCTCCCTGTC R-TCTTTCTTCGGCAAATTCCTG	Real-time PCR	
mACTHR	F-GCTCCAAGGATCATTTACTTGC R-CGCCAGGAGGCTTAACATAAC	mP450scc	F-CCAGTGTCCCCATGCTCAAC R-TGCATGGTCCTTCCAGGTCT
GAPDH	F-ACCACAGTCCATGCCATCAC R-TCCACCACCCTGTTGCTGA	mHSD3b1	F-TAACAATTTAACAGCCCCTCCTAAGG R-ATCCAGCCATGGTCAACACA
GFP	F-TGACCACCCTGACCTACGGCGT R-GGTAGTGGTTGTCGGGCAGCA	mHSD3b6	F-AAACCATCCTCCACTGTTCTAGCT R-TGGAGATGGTCAGCCACAAG
mHSD17b3	F-ATTTTACCAGACAAGACATCT R-GGGGTCAGCACCTGAATAATG	mP450c17	F-AGTTTGCCATCCCGAAGGA R-CTGGCTGGTCCATTCATTT
mP450aro	F-TCAATACCAGGTCCTGGCTA R-GTATGCACTGATTCACGTTC	mHSD17b3	F-TGGGACAATGGGCAGTGAT R-GCCAACTCAAATGAATAGGCTTTC
hStAR	F-GAGAGTCAGCAGGACAATGG R-CTGGTTGATGATGCTCTTGG	β-Actin	F-CAACCGTGAAAAGATGACCCAGATC R-AGTCCATCACAATGCCTGTGGTAC
hP450scc	F-TAGTGTCTCCTTGATGCTGG R-GAAAGGAAGTGTTCACCACG		

F, Forward; R, reverse.

the steroidogenic lineage, we first introduced a human CYP11A1 promoter/GFP gene construct into the mMSCs. This was accomplished by using a 2.3-kb fragment of the promoter region of the human CYP11A1 (a gene that encodes cytochrome P450scc, cholesterol side-chain cleavage enzyme), which has been shown to selectively drive transgene expression to adrenal and gonadal steroidogenic cells (17). In some of the transformed cell lines, GFP fluorescence was detected, as shown in Fig. 2, B and C, but the number of GFP-expressing cells was very low. Thus, GFP-positive cells were enriched by sorting with flow cytometry (Fig. 2E, 1–5% of total cells). As shown in Fig. 2, F and G, enriched GFP-positive cells were also positive for P450scc, indicating that a very small but distinct portion of the mMSCs had spontaneously differentiated into cells that produce the steroid hormone-synthesizing enzyme. Further analysis of the differentiated cells revealed the expression of several genes that are specific to testicular Leydig cells, as shown in Fig. 2H. These include a nuclear orphan receptor SF-1, 3β-HSD types I and VI, and LH receptor (Fig. 2H, lane SCC+). LH receptor and 3β-HSD VI are known to be typical markers for androgen producing cells, such as Leydig cells (25). These observations further support the *in vivo* findings that rodent MSCs have the capacity to differentiate into Leydig-like cells in the testis.

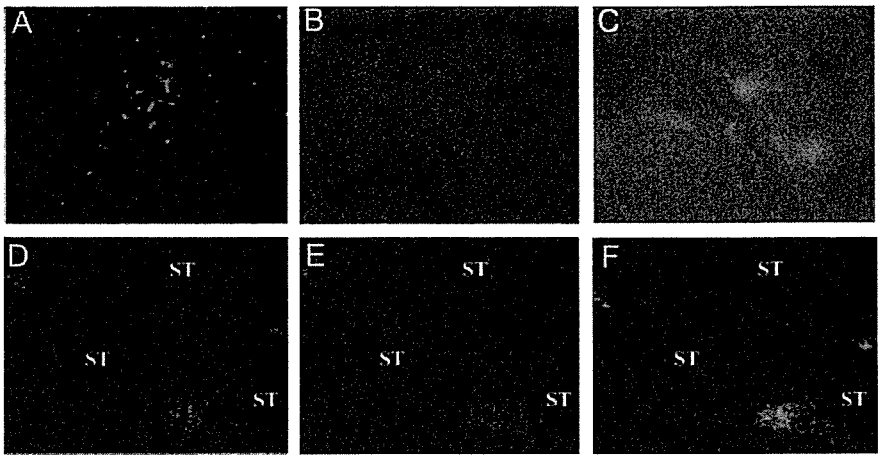

FIG. 1. Transplantation of GFP-positive MSCs into the testis. A, Fluorescence view of MSCs from a green rat 3 d after the first passage. Fluorescence microscopic view of testis before (B) or 3 wk after (C) MSC transplantation. Double staining of frozen sections from the testis 5 wk after MSC transplantation with anti-GFP (D) and anti-P450scc (E) antibodies. F, Merged fluorescent image of D and E. ST, Seminiferous tubule.

Stable transfection of SF-1 into mouse MSCs

It is noteworthy that SF-1 expression was induced in the GFP-positive cells (Fig. 2H). SF-1, also known as Ad4BP, regulates the cell-specific expression of a variety of proteins that are involved in steroidogenesis, in addition to its roles in reproduction and gonadal differentiation (26). Therefore, we next examined the effects of the stable transfection of SF-1 to mMSCs. Various cell lines that stably express SF-1 were isolated. As shown in Fig. 3C, SF-1-induced morphological changes in the cells, such as the accumulation of numerous lipid droplets. However, the transformed cells did not express steroidogenic enzyme genes or produce any steroid

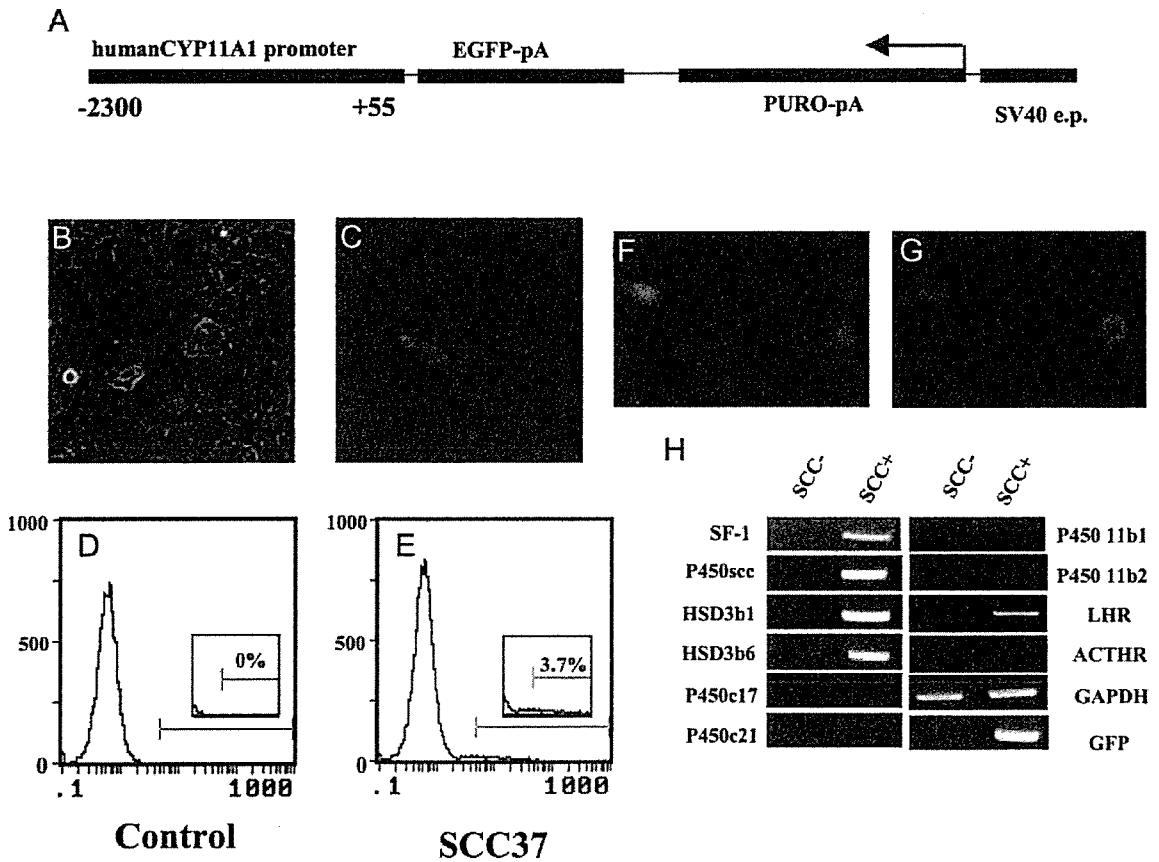

FIG. 2. Spontaneous differentiation of KUM9 into steroidogenic cells. A, Schematic representation of the SCC-reporter gene (SCC-GFP). The SCC-GFP reporter plasmid contains the 2300-bp upstream sequence of the human CYP11A1 gene and the puromycin-*N*-acetyltransferase gene (PURO-pA) driven by the Simian virus 40 early promoter (SV40 e.p.). Phase-contrast (B) and fluorescent (C) images of mMSCs transfected with SCC-GFP and selected by puromycin are shown. Flow cytometric analysis of enhanced GFP (EGFP) expression in KUM9 transfected with control-GFP (D) or SCC-GFP (E) are shown. KUM9-derived cells expressing GFP (F) under the control of the human CYP11A1 promoter were immunocytochemically stained with anti-P450scc antibody (G). H, SCC-GFP-positive (SCC+) and negative (SCC−) populations were sorted and analyzed for various marker genes by RT-PCR.

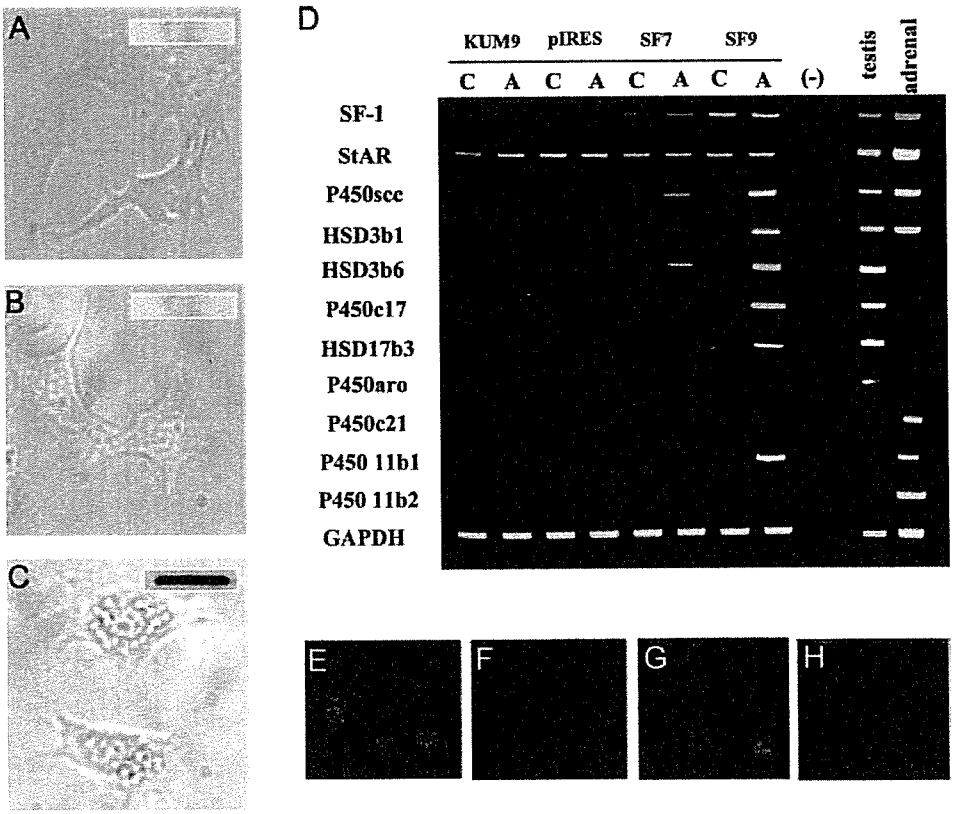

FIG. 3. Differentiation of KUM9 into steroidogenic cells. Phase-contrast images of mMSCs untransfected (A) or stably transfected with the control (B) or the SF-1-expression (C) vectors are shown. An immunoblot analysis was performed with an antibody against SF-1 (*insets*). D, RT-PCR analysis of each clones cultured with or without 8-bromoadenosine-cAMP (8br-cAMP) for 7 d (C: without 8br-cAMP; A: with 8br-cAMP). Data were compared with those from mouse adrenal and testicular tissues. Fluorescent images of 4′,6′-diamino-2-phenylindole staining (E and G) and a P450scc immunostaining (F and H) of KUM9 transfected with the SF-1-expressing vector and then cultured with (G and H) or without 8br-cAMP (E and F).

hormones (Fig. 3D and Table 2). Therefore, we next added cAMP to the cultures because cAMP is known to induce steroidogenesis in a number of steroidogenic cell lines. Treatment of confluent cultures with cAMP was found to induce both P450scc mRNA (Fig. 3D) and protein (Fig. 3H) in the transformed cell lines, SF7 and SF9, whereas no induction was observed in untransfected (KUM9) or vector-transfected (pIRES) mMSCs (Fig. 3D). Treatment of the cells for a period of 7 d further induced the expression of other steroidogenic enzyme genes, as shown in Fig. 3D. Several cell lines showed similar expression patterns (two of which are shown in Fig. 3D).

3β-HSD types I and VI were induced 3 d after cAMP treatment (Fig. 4). In the testis, the formation of testosterone is dependent on 3β-HSD activity, and isoform types I and VI have been shown to be expressed in the adult mouse testis (27). P450c17 and 17β-hydroxysteroid dehydrogenase III (17β-HSD III) were induced 5 d after the treatment (Fig. 4). It is interesting to note that the order of induction of the enzymes is similar to the sequential order for the steroid hormone synthetic pathway. 3β-HSD enzymes are essential for the production of progesterone, and P450c17 and 17β-HSD III are both required for the production of testosterone in testicular Leydig cells. Consistent with the expression pattern of the steroidogenic enzymes, testosterone was the major sex steroid hormone produced in the transformed cell line, SF9, when treated with cAMP for 7 d (Table 2). Two adrenal-specific steroid hormones, glucocorticoids and mineralocorticoids, were not detected in these cells. These results clearly demonstrate that the stable expression of SF-1 and the addition of cAMP induced the differentiation of mMSCs into steroidogenic cells and that these cells have properties that are similar to those of testicular Leydig cells.

TABLE 2. Production of steroid hormones by MSCs stably expressing SF-1 (SF9-KUM9 or SF4-hMSC) in the presence (+) or absence (−) of 8br-cAMP (ng/ml)

Cell (cAMP)	Progesterone	Testosterone	Estradiol	Glucocorticoid	Aldosterone
pIRES-KUM9 (−)	N.D.	N.D.	N.D.	N.D.	N.D.
pIRES-KUM9 (+)	N.D.	N.D.	N.D.	N.D.	N.D.
SF9-KUM9 (−)	N.D.	N.D.	N.D.	N.D.	N.D.
SF9-KUM9 (+)	24.3 ± 4.25	1.6 ± 0.29	N.D.	N.D.	N.D.
pIRES-hMSC (−)	N.D.	N.D.	N.D.	N.D.	N.D.
pIRES-hMSC (+)	N.D.	N.D.	N.D.	N.D.	N.D.
SF4-hMSC (−)	N.D.	N.D.	N.D.	N.D.	N.D.
SF4-hMSC (+)	270 ± 82.5	17.5 ± 0.20	0.21 ± 0.11	520 ± 200	1.56 ± 0.42

Data are means and SEM values of at least duplicate assays. N.D., No detectable values.

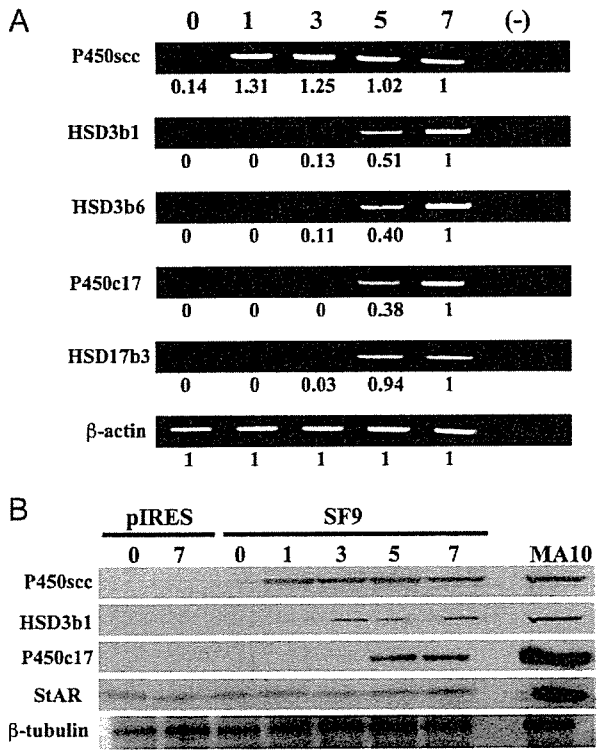

FIG. 4. Time-dependent induction of steroidogenic enzymes by cAMP. KUM9 cells stably transfected with SF-1-expression (SF9) or control (pIRES) vector were cultured and treated with 8-bromoadenosine-cAMP for the indicated times. A, P450scc, 3β-HSD I, 3β-HSD VI, P450c17, and 17β-HSD III mRNA levels were analyzed by RT-PCR and real-time PCR. Real-time PCR data are the mean values of at least triplicate assays. The 7-d value was arbitrarily taken as 1.0. B, Immunoblot analyses were performed with antibodies against StAR, P450scc, 3β-HSD I, P450c17, and β-tubulin using the same lysates. The data were compared with that from MA-10 cells treated with cAMP (4 h).

Stable transfection of SF-1 into human MSCs

We next examined the issue of whether the same approach could also be used to induce the differentiation of human MSCs (hMSCs) into steroidogenic cells. Similar to the results obtained with mMSCs, hMSCs (hMSC-TERT-E6/E7) expressed no steroidogenic enzymes or StAR before transfection with SF-1 even after cAMP treatment (Fig. 5). After SF-1 transfection, all the transformed cell lines became positive for StAR gene expression, and the expression levels were further increased by cAMP treatment. Most of the steroidogenic enzymes, P450scc, 3β-HSD II, P450c17, cytochrome P450 steroid 21-hydroxylase (P450c21), cytochrome P450 aromatase (P450arom), and cytochrome P450 steroid 11 β-hydroxylase, were also substantially induced by cAMP stimulation. A significant difference between mMSCs and hMSCs was the strong expression of the P450c21 gene in the case of hMSCs. This caused a difference in the kinds of steroids produced by mMSCs and hMSCs. As listed in Table 2, glucocorticoids were the major steroids produced by the transformed hMSCs, hSF4, whereas testosterone was the major product from the transformed mMSCs, mSF9. The hSF4 cells mainly produced cortisol, the major glucocorticoid produced by the human adrenal gland. These results clearly demonstrate that the stable expression of SF-1 and subsequent cAMP treatment induced the differentiation of hMSCs into steroidogenic cells. In addition, the cortisol-producing cells also expressed ACTH receptors and can respond to ACTH for the quick production of cortisol at nanomolar levels (data not shown).

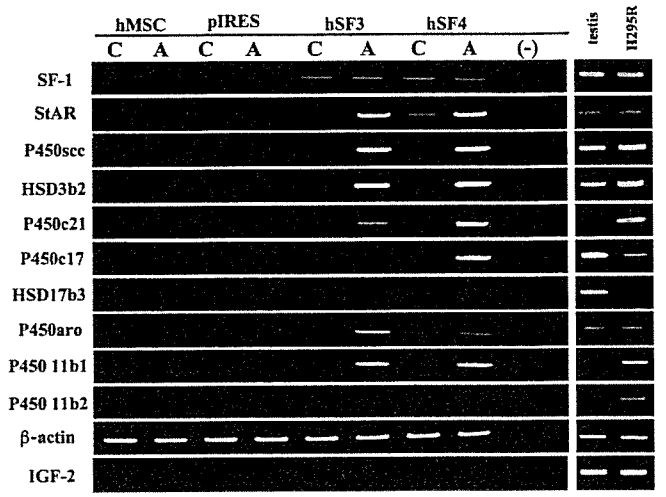

FIG. 5. Induction of steroidogenic enzymes in hMSCs. hMSCs were stably transfected with the control (pIRES) or SF-1-expression (SF3, -4) vector. RT-PCR analysis of each clone was cultured with or without 8-bromoadenosine-cAMP (8br-cAMP) for 7 d (C: without 8br-cAMP; A: with 8br-cAMP). The data were compared with that from human testis and NCI-H295R, a human adrenocortical tumor cell line, treated with cAMP (24 h).

Human MSCs also expressed P450arom as in the case of the human adrenocortical carcinoma NCI-H295R cell line (Fig. 5), whereas normal adrenal cells do not express it (28). However, hSF3 or -4 did not express IGF-II, an adrenocortical tumor marker. It has recently been shown that P450arom is expressed in human bone marrow stroma cells under certain conditions (29). Thus, it is probable that the expression of P450arom in hMSCs was not the result of a malignant phenotype or the differentiation of the cells by SF-1 and cAMP treatment.

Stable transfection of SF-1 into cells other than MSCs

We next examined the effects of transfection of SF-1 into several cell lines other than MSCs, *i.e.* a human cell line HEK293, murine embryonic stem cells, and murine cell lines F9 and NIH3T3. None of the transfected cell lines autonomously produced steroid hormones, although some were induced to express the P450scc and 3β-HSD genes (Fig. 6).

Discussion

The findings presented herein demonstrate that rodent MSCs have the potential to differentiate into steroidogenic cells with characteristics that are very similar to testicular Leydig cells. It has been postulated that mesenchymal progenitors of Leydig cells are present in the testicular interstitium (12). Immature Leydig cells are gradually replaced by mature Leydig cells that are thought to differentiate from these mesenchymal progenitors during the prepubertal period. In fact, the injection of MSCs into the testis during this critical period caused the differentiation of MSCs into steroidogenic cells that were indistinguishable from Leydig cells. Concerning the *in vivo* experiments, the possibility of

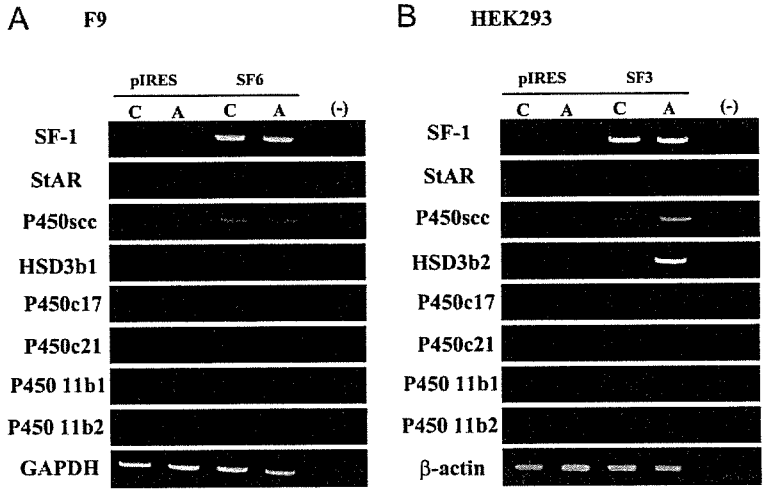

FIG. 6. Stable transfection of SF-1 and cAMP treatment for F9 (A) and HEK293 cells (B). RT-PCR analysis of steroidogenesis-related genes in each stable cell line transfected with SF-1 or pIRES (control) cultured with or without 8-bromoadenosine-cAMP (8br-cAMP) for 7 d (C: without 8br-cAMP; A: with 8br-cAMP).

cell fusion between donor MSCs and recipient testicular Leydig cells or their progenitor cells cannot be excluded. However, it should be emphasized that very small but distinct portions of mMSCs underwent spontaneous differentiation into Leydig-like cells *in vitro*. Lo *et al.* (30) demonstrated, by means of a cell transplantation assay, the presence of stem cells or progenitors for Leydig cells. Therefore, our data strongly suggest that bone marrow-derived MSCs share common properties with testicular MSCs or Leydig cell progenitors. Conversely, testicular MSCs or Leydig cell progenitors might also have pluripotent characteristics, similar to bone marrow-derived MSCs, as has been reported for some other MSCs (4, 31).

In addition, transfection of cultured mMSCs with SF-1 followed by cAMP stimulation resulted in their differentiation into Leydig cells. The same procedure also led to the successful induction of hMSCs into steroidogenic cells. In this case, however, most of the cell lines expressing SF-1 largely produced glucocorticoids rather than testosterone. This was mainly due to the strong induction of P450c21 gene expression in the hMSCs. To investigate the issue of whether hMSCs are able to differentiate into Leydig cells, we also injected hMSCs to the testis of nude mice or rats (data not shown). Unfortunately, the human cells did not survive for more than several weeks in the rodent testis.

Because the established cell lines need much longer times than general steroidogenic cells to produce steroid hormones by cAMP stimulation in this study, we speculate that cAMP treatment of this study is necessary for the induction of the cellular differentiation rather than direct stimulation of gene transcription of steroidogenic enzymes.

In hMSCs, the stable expression of SF-1 and cAMP treatment induced the expression of the StAR gene, which is essential for the transfer of cholesterol from the outer to the inner membrane of mitochondria in which the conversion of cholesterol to steroid hormones begins (21). The same treatment failed to induce StAR gene expression in several cell lines (other than MSCs) including embryonic stem (ES) cells and therefore failed to induce any steroid hormones. The expression of the P450scc or 3β-HSD gene was induced at low levels in some of them, however (Fig. 6). It has been reported that the stable transfection of SF-1 into ES cells results in morphological changes and the induction of P450scc enzyme expression, (32). No autonomous production of steroid hormones was observed, however, probably because of the deficiency of cholesterol storage and mobilization and the lack of StAR protein expression (32). Therefore, our present observations suggest that MSCs, but not ES cells, are excellent precursors of steroidogenic cells. In contrast to human cells, StAR was constitutively expressed in KUM9 as well as the freshly isolated rat MSCs (our unpublished data). Therefore, we speculate that StAR gene expression is not always under the control of SF-1, and the pattern of expression may be different between species, even in the same tissues. In addition to the steroidogenesis, the movement of cholesterol to the inner mitochondrial membrane is also important for its metabolism, because one of the rate-determining steps, the 27-hydroxylation of cholesterol, is catalyzed by sterol 27-hydroxylase, which is located in the inner mitochondrial membrane (33, 34). Cholesterol metabolites, such as oxysterols have been proposed to be potential regulators of genes in cholesterol homeostasis (33). We found that sterol 27-hydroxylase mRNA was detectable in rat and mouse MSCs (data not shown), suggesting that it is involved in cholesterol metabolism. Therefore, it is assumed that the StAR protein in KUM9 is present to promote the cholesterol metabolism, despite the fact that steroidogenesis does not take place. In support of this hypothesis, ectopic expression of the StAR protein increases the metabolism of cholesterol in rat primary hepatocytes (34).

Gondo *et al.* (35) recently reported that the adenovirus-mediated forced expression of SF-1 transforms primary long-term cultured murine bone marrow cells into ACTH-responsive steroidogenic cells. In contrast to our observation obtained from murine MSCs, their steroidogenic cells produce both gonadal and adrenal steroids. There are two possible explanations for their results: 1) their cells were a mixed adrenal/gonadal phenotype or 2) were a mixture of adrenal or gonadal phenotypic cells. The latter seems to be more likely because our study clearly demonstrated the differentiation of adult stem cells derived from both murine and human into gonadal or adrenal steroidogenic cells. Therefore, with respect to the difference between mouse and human cells, we assume that the mouse MSCs used in our study were already committed to the gonadal lineage, whereas the hMSCs were already committed to

the adrenal lineage. In support of this hypothesis, it has frequently been reported that MSCs are heterogeneous populations that have a different differentiation potential (1, 2, 10). In a future study, the same treatment of various mouse or human MSCs need to be carried out, followed by observations of whether both adrenal and gonadal phenotypes are obtained. This might also provide a tool for revealing the pathway leading to the differentiation of the cells into adrenal or gonadal steroidogenic cells.

In summary, we demonstrate here that MSCs have the capacity to differentiate into steroidogenic cells, both *in vivo* and *in vitro*. MSCs represent not only a powerful tool for studies of the differentiation of the steroidogenic lineage but may also offer a possible clinical stem cell resource for diseases of steroidogenic organs.

Acknowledgments

We are grateful to Drs. K. Morohashi, W. Miller, B. C. Chung, A. Payne, and D. Hales for providing plasmids and antisera. We also thank Drs. M. Ascoli and J. Toguchida for the generous gifts of MA10 and hMSCs and Ms. Y. Inoue, T. Satake, and K. Matsuura for technical assistance.

Received February 8, 2006. Accepted May 16, 2006.

Address all correspondence and requests for reprints to: Kaoru Miyamoto, Department of Biochemistry, Faculty of Medical Sciences, University of Fukui, Shimoaizuki, Matsuoka-cho, Fukui 910-1193, Japan. E-mail: kmiyamot@fmsrsa.fukui-med.ac.jp.

This work was supported in part by a grant from the Smoking Research Foundation and the 21st Century Center of Excellence Program (Medical Science).

All authors (T.Y., T.M., K.Y., H.K., T.S., M.Y., T.K., Z.S., A.U., K.M.) have nothing to declare.

References

1. **Friedenstein AJ, Gorskaja JF, Kulagina NN** 1976 Fibroblast precursors in normal and irradiated mouse hematopoietic organs. Exp Hematol 4:267–274
2. **Prockop DJ** 1997 Marrow stromal cells as stem cells for nonhematopoietic tissues. Science 276:71–74
3. **Ferrari G, Cusella-De Angelis G, Coletta M, Paolucci E, Stornaiuolo A, Cossu G, Mavilio F** 1998 Muscle regeneration by bone marrow-derived myogenic progenitors. Science 279:1528–1530
4. **Lee OK, Kuo TK, Chen WM, Lee KD, Hsieh SL, Chen TH** 2004 Isolation of multipotent mesenchymal stem cells from umbilical cord blood. Blood 103: 1669–1675
5. **D'Amour KA, Gage FH** 2003 Genetic and functional differences between multipotent neural and pluripotent embryonic stem cells. Proc Natl Acad Sci USA 100(Suppl 1):11866–11872
6. **De Ugarte DA, Morizono K, Elbarbary A, Alfonso Z, Zuk PA, Zhu M, Dragoo JL, Ashjian P, Thomas B, Benhaim P, Chen I, Fraser J, Hedrick MH** 2003 Comparison of multi-lineage cells from human adipose tissue and bone marrow. Cells Tissues Organs 174:101–109
7. **Kopen GC, Prockop DJ, Phinney DG** 1999 Marrow stromal cells migrate throughout forebrain and cerebellum, and they differentiate into astrocytes after injection into neonatal mouse brains. Proc Natl Acad Sci USA 96:10711–10716
8. **Ortiz LA, Gambelli F, McBride C, Gaupp D, Baddoo M, Kaminski N, Phinney DG** 2003 Mesenchymal stem cell engraftment in lung is enhanced in response to bleomycin exposure and ameliorates its fibrotic effects. Proc Natl Acad Sci USA 100:8407–8411
9. **Chamberlain JR, Schwarze U, Wang PR, Hirata RK, Hankenson KD, Pace JM, Underwood RA, Song KM, Sussman M, Byers PH, Russell DW** 2004 Gene targeting in stem cells from individuals with osteogenesis imperfecta. Science 303:1198–1201
10. **Prockop DJ, Gregory CA, Spees JL** 2003 One strategy for cell and gene therapy: harnessing the power of adult stem cells to repair tissues. Proc Natl Acad Sci USA 100(Suppl 1):11917–11923
11. **Hatano O, Takakusu A, Nomura M, Morohashi K** 1996 Identical origin of adrenal cortex and gonad revealed by expression profiles of Ad4BP/SF-1. Genes Cells 1:663–671
12. **Roosen-Runge EC, Anderson D** 1959 The development of the interstitial cells in the testis of the albino rat. Acta Anat (Basel) 37:125–137
13. **Holmes PV, Dickson AD** 1971 X-zone degeneration in the adrenal glands of adult and immature female mice. J Anat 108:159–168
14. **Pochampally RR, Neville BT, Schwarz EJ, Li MM, Prockop DJ** 2004 Rat adult stem cells (marrow stromal cells) engraft and differentiate in chick embryos without evidence of cell fusion. Proc Natl Acad Sci USA 101:9282–9285
15. **Makino S, Fukuda K, Miyoshi S, Konishi F, Kodama H, Pan J, Sano M, Takahashi T, Hori S, Abe H, Hata J, Umezawa A, Ogawa S** 1999 Cardiomyocytes can be generated from marrow stromal cells in vitro. J Clin Invest 103:697–705
16. **Okamoto T, Aoyama T, Nakayama T, Nakamata T, Hosaka T, Nishijo K, Nakamura T, Kiyono T, Toguchida J** 2002 Clonal heterogeneity in differentiation potential of immortalized human mesenchymal stem cells. Biochem Biophys Res Commun 295:354–361
17. **Hu MC, Chou SJ, Huang YY, Hsu NC, Li H, Chung BC** 1999 Tissue-specific, hormonal, and developmental regulation of SCC-LacZ expression in transgenic mice leads to adrenocortical zone characterization. Endocrinology 140: 5609–5618
18. **Mizutani T, Yamada K, Yazawa T, Okada T, Minegishi T, Miyamoto K** 2001 Cloning and characterization of gonadotropin-inducible ovarian transcription factors (GIOT1 and -2) that are novel members of the (Cys)(2)-(His)(2)-type zinc finger protein family. Mol Endocrinol 15:1693–1705
19. **Rutledge RG, Cote C** 2003 Mathematics of quantitative kinetic PCR and the application of standard curves. Nucleic Acids Res 31:e93
20. **Yazawa T, Mizutani T, Yamada K, Kawata H, Sekiguchi T, Yoshino M, Kajitani T, Shou Z, Miyamoto K** 2003 Involvement of cyclic adenosine 5′-monophosphate response element-binding protein, steroidogenic factor 1, and Dax-1 in the regulation of gonadotropin-inducible ovarian transcription factor 1 gene expression by follicle-stimulating hormone in ovarian granulosa cells. Endocrinology 144:1920–1930
21. **Bose HS, Whittal RM, Baldwin MA, Miller WL** 1999 The active form of the steroidogenic acute regulatory protein, StAR, appears to be a molten globule. Proc Natl Acad Sci USA 96:7250–7255
22. **Hu MC, Guo IC, Lin JH, Chung BC** 1991 Regulated expression of cytochrome P-450scc (cholesterol-side-chain cleavage enzyme) in cultured cell lines detected by antibody against bacterially expressed human protein. Biochem J 274(Pt 3):813–817
23. **Hales DB, Sha LL, Payne AH** 1987 Testosterone inhibits cAMP-induced *de novo* synthesis of Leydig cell cytochrome P-450(17α) by an androgen receptor-mediated mechanism. J Biol Chem 262:11200–11206
24. **Medvinsky A, Smith A** 2003 Stem cells: fusion brings down barriers. Nature 422:823–825
25. **O'Shaughnessy PJ, Willerton L, Baker PJ** 2002 Changes in Leydig cell gene expression during development in the mouse. Biol Reprod 66:966–975
26. **Parker KL, Schimmer BP** 1997 Steroidogenic factor 1: a key determinant of endocrine development and function. Endocr Rev 18:361–377
27. **Peng L, Arensburg J, Orly J, Payne AH** 2002 The murine 3β-hydroxysteroid dehydrogenase (3β-HSD) gene family: a postulated role for 3β-HSD VI during early pregnancy. Mol Cell Endocrinol 187:213–221
28. **Staels B, Hum DW, Miller WL** 1993 Regulation of steroidogenesis in NCI-H295 cells: a cellular model of the human fetal adrenal. Mol Endocrinol 7:423–433
29. **Heim M, Frank O, Kampmann G, Sochocky N, Pennimpede T, Fuchs P, Hunziker W, Weber P, Martin I, Bendik I** 2004 The phytoestrogen genistein enhances osteogenesis and represses adipogenic differentiation of human primary bone marrow stromal cells. Endocrinology 145:848–859
30. **Lo KC, Lei Z, Rao Ch V, Beck J, Lamb DJ** 2004 *De novo* testosterone production in luteinizing hormone receptor knockout mice after transplantation of Leydig stem cells. Endocrinology 145:4011–4015
31. **De Bari C, Dell'Accio F, Tylzanowski P, Luyten FP** 2001 Multipotent mesenchymal stem cells from adult human synovial membrane. Arthritis Rheum 44:1928–1942
32. **Crawford PA, Sadovsky Y, Milbrandt J** 1997 Nuclear receptor steroidogenic factor 1 directs embryonic stem cells toward the steroidogenic lineage. Mol Cell Biol 17:3997–4006
33. **Bjorkhem I** 2002 Do oxysterols control cholesterol homeostasis? J Clin Invest 110:725–730
34. **Pandak WM, Ren S, Marques D, Hall E, Redford K, Mallonee D, Bohdan P, Heuman D, Gil G, Hylemon P** 2002 Transport of cholesterol into mitochondria is rate-limiting for bile acid synthesis via the alternative pathway in primary rat hepatocytes. J Biol Chem 277:48158–48164
35. **Gondo S, Yanase T, Okabe T, Tanaka T, Morinaga H, Nomura M, Goto K, Nawata H** 2004 SF-1/Ad4BP transforms primary long-term cultured bone marrow cells into ACTH-responsive steroidogenic cells. Genes Cells 9:1239–1247

Endocrinology is published monthly by The Endocrine Society (http://www.endo-society.org), the foremost professional society serving the endocrine community.

Original Paper

nephron
Experimental
Nephrology

Nephron Exp Nephrol 2006;104:e63–e75
DOI: 10.1159/000093999

Received: February 7, 2006
Accepted: March 30, 2006
Published online: June 19, 2006

Leucine-Rich Repeat-Containing G Protein-Coupled Receptor-4 (LGR4, Gpr48) Is Essential for Renal Development in Mice

Shigeki Kato[a] Mitsunobu Matsubara[b] Tsuyoshi Matsuo[a] Yasuaki Mohri[a]
Itsuro Kazama[b] Ryo Hatano[b] Akihiro Umezawa[c] Katsuhiko Nishimori[a]

[a]Laboratory of Molecular Biology, Graduate School of Agricultural Science, Tohoku University, Sendai, [b]Division of Molecular Medicine, Center for Translational and Advanced Animal Research, Tohoku University School of Medicine, Sendai, and [c]National Research Institute for Child Health and Development, Tokyo, Japan

Key Words
G protein-coupled receptor, leucine-rich repeat-containing · Glycoprotein hormone receptor homology · Leucine-rich repeats · Renal hypoplasia

Abstract
Leucine-rich repeat-containing G protein-coupled receptor (LGR)-4 is a G protein-coupled receptor (GPCR) with a seven-transmembrane domain structure. LGRs are evolutionally and structurally phylogenetic, classified into three subgroups and are members of the so-called orphan receptors whose ligands have yet to be identified. We generated knockout mice lacking *Lgr4 (Gpr48)* by targeted deletion of part of exon 18, which codes for the transmembrane and signal-transducing domains of the receptor. *Lgr4* null mice were born at much less than the 25% expected frequency from crosses of *Lgr4* heterozygous mice *(Lgr4$^{+/-}$)*. *Lgr4* null mice that survived in utero died shortly after birth in almost all cases. We observed striking renal hypoplasia in the null mice, accompanied by elevated concentration of plasma creatinine. Histological analysis of the P0 null mouse kidney showed a notable decrease in the total number and density of the glomerulus. Thus, the function of *Lgr4* is essential to regulate renal development in the mouse. This study suggests that the *Lgr4* gene is a new and important member of LGRs involved in a group of genes responsible for hereditary disease in the kidney.

Introduction

Leucine-rich repeat-containing G protein-coupled receptor 4 *(Lgr4; Gpr48)* was first identified as a novel G protein-coupled receptor with glycoprotein hormone receptor homology [1]. Glycoprotein hormone receptors, including the gonadotropin receptors follicle-stimulating hormone receptor [2] and luteinizing hormone/chorionic gonadotropin receptor [3], share conserved leucine-rich repeats in their first extracellular domains. These extracellular domains typically comprise more than half of the total protein amino acids. The receptors couple with intracellular Gsα-type G proteins, and their intracellular effects are mediated in large part by adenylate cyclase activity and the resulting increase in cellular cAMP levels. Although *LGR7* [4, 5] and *LGR8* [6, 7] were recently identified as receptors for relaxin [8–10], ligands for many other newly identified LGRs, including LGR4, are unknown; hence, LGR4 is classified among the orphan receptors. Ligands of the most well-characterized receptors, including follicle-stimulating hormone, luteinizing hormone, human chorionic gonadotropin, and thyroid-stimulating hormone, are heterodimeric in composition, consisting of the common α-subunit and the hormone-specific β-subunit. Ligands of the still orphan LGRs are presumed to be structurally related.

Mice deficient in the *Lgr4* gene are a potentially valuable tool to study the in vivo function of *Lgr4* and to ex-

KARGER

Fax +41 61 306 12 34
E-Mail karger@karger.ch
www.karger.com

1660–2129/06/1042–0063$23.50/0

Accessible online at:
www.karger.com/nee

Katsuhiko Nishimori
Laboratory of Molecular Biology, Graduate School of Agricultural Science
Tohoku University, 1-1 Tsutsumidori-Amamiyamachi, Aoba-ku
Sendai 981-8555 (Japan)
Tel. +81 22 717 8770, Fax +81 22 717 8883, E-Mail knishimo@mail.tains.tohoku.ac.jp

plore LGR4 candidate ligand(s). To address the physiological roles of mouse *Lgr4*, we deleted a part of exon 18 coding for the transmembrane and signal-transducing domains of LGR4 via homologous recombination in embryonic stem (ES) cells. We describe this herein, as well as our characterization of renal developmental phenotypes in *Lgr4* null mutant mice.

Materials and Methods

Northern Blot Analysis

Messenger RNA was extracted from different organs using RNA Stat 60 (Leedo Medical Laboratories, USA). Two micrograms of poly(A)+ RNA were electrophoresed, transferred onto nylon transfer membrane (Pall BioSupport, USA), and blocked before being used for hybridization. A [^{32}P]-dCTP-radiolabeled probe was generated from 440 bp of sequence corresponding to nucleotide (nt) 101 to 540 of mouse *Lgr4* mRNA (Amersham Biosciences, Japan) and applied to the blot under standard hybridization conditions. After washing, the blot was exposed to X-ray film (Kodak, Japan). The size of the transcripts was estimated using the positions of 18S rRNA, 28S rRNA and GAPD mRNA.

5′ Primer Extension Analysis

Primer extension analysis was performed. Briefly, an IRD-800 (LI-COR, Japan)-labeled oligonucleotide complementary to bases from nt –211 to –193 of the coding strand (5′-GAAGGGAGAAACTGCGGAG-3′) was hybridized overnight at 42°C with 15 μg total RNA from mouse ovaries. Hybridized samples were reverse transcribed into cDNA with Superscript III Reverse Transcriptase (Invitrogen, Japan). One microgram of RNase H (Invitrogen, Japan) was added, and the reaction was incubated at 37°C for 30 min. The resultant products were precipitated and run on a 6% denaturing polyacrylamide gel along with the corresponding sequence reactions.

Generation of Lgr4-Deficient Mice

The genomic targeting vector contained, in order, 7.5 kb of genomic sequence (including *Lgr4* exons 11–17), a 5′-*lox*P site, a PgkNeo-expression cassette surrounded by FRT sites at both ends, a portion of exon 18, a 3′-*lox*P site, and 2.0 kb of genomic DNA downstream of the *Lgr4*-coding region (including an untranslated *Lgr4* mRNA sequence). An expression cassette for negative selection of non-homologous insertion MC1-tk was also added. E14Tg2a ES cells were electroporated with 25 μg of linearized targeting vector, and targeted clones were selected for using G418 and 1-(2-deoxy-2-fluoro-β-D-arabinofuranosyl)-5-iodouracil (FIAU; Moravek Biochemicals, USA). Clones with the desired homologous recombination events at both sides of the vector were identified by Southern blot analysis using a 5′-internal probe and 3′-external probe [11]. These ES cell clones were used for C57BL/6 blastocyst injection to generate germline transmission chimeras. We defined the $Lgr4^{Floxed}$ allele as that with the intact targeting vector, and maintained heterozygous $Lgr4^{Floxed}$ mice ($Lgr4^{Floxed/+}$) in a mixed 129 SvEvC57BL/6 genetic background. To obtain the *Lgr4* knockout or null allele, $Lgr4^{Floxed/+}$ mice were crossed with CAG-Cre 'transgenic general deleter' mice [12]. Heterozygous mice ($Lgr4^{+/-}$) were then interbred to produce the null mice (fig. 3A). The Ethics Review Committee for Animal Experimentation of Tohoku University approved all experimental protocols described in the present study.

PCR Genotyping

PCR analysis was used for genotyping DNA obtained from tail samples. Genomic DNA was extracted by ethanol precipitation after proteinase K digestion in a tissue lysis buffer (50 mM Tris-HCl (pH 7.5), 50 mM EDTA (pH 8.0), 100 mM NaCl, 0.5 mM spermidine, 1% SDS, 5 mM DTT). Three primers were used to distinguish the mutated allele from the wild-type allele; they were designated: upstream primer 1 (5′-GCCACAAGGGAGGATAGAATC-3′), upstream primer 2 (5′-CCCAGCAAGAGCTAGGAAGA-3′), and downstream primer 3 (5′-GCCATCAAATCCCTTGGATA-3′). The wild-type allele gives a PCR amplicon of 608 bp using primers 1 and 3, while primers 2 and 3 generate a 345-bp product from the null allele.

Fertility Studies

We carried out timed mating by housing one male with one or two females for periods of at least 5 days. Every morning during this period, females were evaluated for the presence of vaginal plug. Embryonic gestation day 0.5 (E0.5) was defined by the presence of a copulation plug, whereas the day of birth was defined as P0. Pregnant heterozygous mice were sacrificed and fetuses were obtained at specific time points in embryonic development, E13.5, 14.5, 15.5, 16.5, 17.5, 18.5, and 19.5. Fetuses and newborns were weighed and sacrificed by decapitation to obtain tails for genotyping and kidneys for histological analysis. Blood was collected from the carotid arteries into 50 μl non-heparinized capillary tubes.

Histology

For renal histology, kidneys from postnatal mice were fixed in 4% paraformaldehyde overnight. After dehydration, they were embedded in paraffin. Paraffin blocks were sectioned at 2- to 5-μm thickness, and stained with hematoxylin-eosin, periodic acid-Schiff (PAS) and periodic acid silver-methenamine using standard procedures. In case of E13.5 kidneys, these were frozen with Tissue-Tek O.C.T. Compound (Sakura Finetechnical, Japan), sectioned at 6–10 μm, fixed, and further processed as described for the postnatal kidneys.

Blood Analysis

Plasma creatinine levels were measured by a chemical autoanalyzer (DRI-CHEM 3500V, Fuji Film, Japan). Breathing neonatal mice were decapitated and about 20 μl of blood was immediately corrected by a pipetteman. The blood sample was centrifuged (3,000 rpm) for 5 min at room temperature to prepare supernatant as plasma. Ten microliters of plasma sample were further processed with the autoanalyzer according to the manufacturer's protocol.

Nephron Density Studies

The numbers of nephrons per unit area (mm^3) were counted. For each kidney collected, three ($Lgr4^{-/-}$) or four ($Lgr4^{+/+}$ and $Lgr4^{+/-}$) different non-adjacent sections of the organ were used. Data were statistically analyzed.

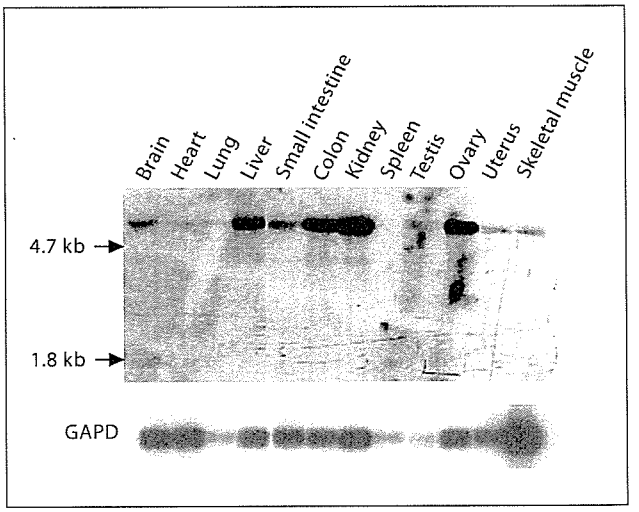

Fig. 1. Multi-tissue Northern blot analysis showing expression of *Lgr4* mRNA. Two micrograms of poly(A)+ RNA from various tissues of adult mice were hybridized with a [α-32P]-labeled 440-bp *Lgr4* cDNA probe. A major message, approximately 5 kb in size, was detected in the kidney, ovary, colon, liver, and brain. The heart, lung, small intestine, testis, uterus and skeletal muscle showed relatively weak signals.

Statistical Evaluation

All experimental data are expressed as the means ± SEM. Individual comparisons were made between genotype groups using ANOVA followed by Student's t test. A p value of <0.05 was considered significant.

Results

Cloning of Lgr4 *cDNA and Tissue Distribution of* Lgr4 *Transcript in Various Organs*

To study the expression of *Lgr4* in wild-type adult mice, we performed Northern blot analysis. As shown in figure 1, a 5.0-kb *Lgr4* transcript was detected in multiple organs. The highest level of expression was seen in the kidney, followed by the ovary, colon, and liver (fig. 1). In contrast, the heart, lung, testis, uterus, and skeletal muscle showed relatively lower signal intensity, and no bands were detected corresponding to transcript in the pancreas or spleen.

Determining the mLgr4 *Transcription Start Site*

To identify the start site of transcription on the m*Lgr4* gene, 5′-primer extension analysis was performed, and we found that transcription was initiated at nt –255 with respect to the translation initiation site (fig. 2). This allows correct description of *Lgr4* exon 1 (440 bp; fig. 3A).

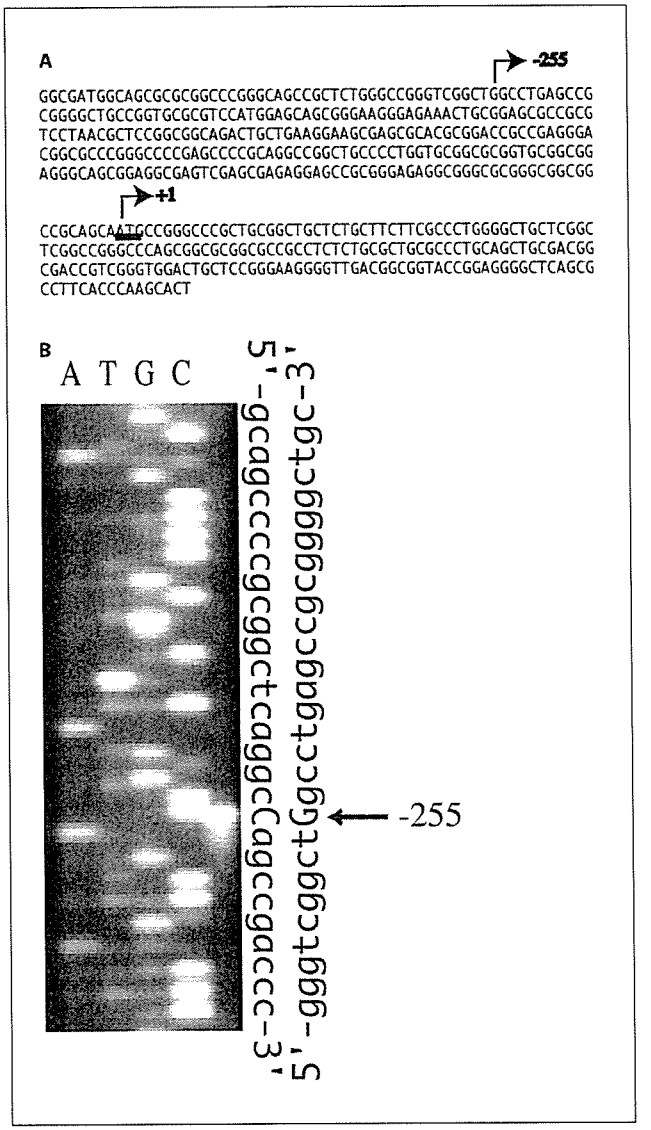

Fig. 2. Determination of the transcription start site of the m*Lgr4* gene. Primer extension analysis with 15 μg of ovary total RNA was done to determine the transcription start site of m*Lgr4*. The band indicates the start site at nt –255 relative to the translational start site.

Construction of the Gene-Targeting Vector and Generation of Lgr4*-Deficient Mice*

To generate a targeting construct, a 7.5-kb fragment spanning from exon 11 to exon 17 was used as a 5′-arm

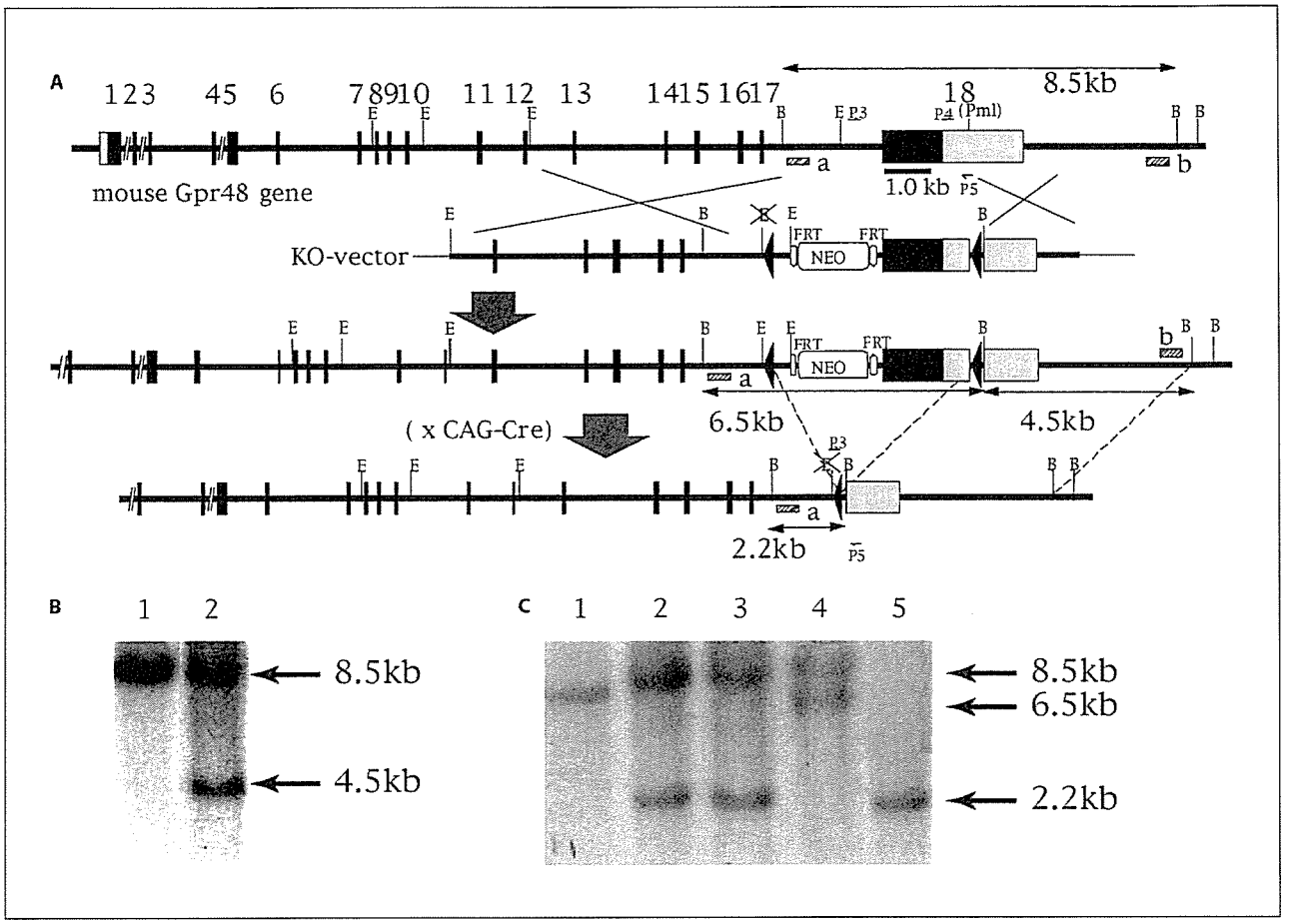

Fig. 3. Construction of the *Lgr4* gene knockout vector, and the generation and characterization of *Lgr4* gene-deficient mice. **A** The wild-type m*Lgr4* allele and the deletion-targeting vector are shown. The targeted domain includes a 2.2-kb sequence comprising half of exon 18. A schema of the targeted allele after homologous recombination and the recombined allele after Cre-mediated excision followed. Black boxes and gray boxes indicate the translated regions and non-translated regions in exons, respectively. Triangles and ellipses are *lox*P and FRT sites, respectively. Exons are numbered. Interruptions within intron-1, intron-2 and intron-4 by double slash lines represent the long intron spanning 52.4, 18.9 and 5.4 kb, respectively. B = *Bam*HI; E = *Eco*RI. **B** Genomic DNA was prepared from ES cell clones and digested with *Bam*HI for analysis by Southern hybridization with probe 'b'. DNA was run on lanes 1 and 2. Lane 1 shows a non-targeted cell and lane 2 shows correct homologous recombination cell. **C** Tail DNA was used for Southern blot hybridization with probe 'a'. The picture shows results for wild-type mice (+/+; lane 1), heterozygous mice (+/−; lanes 2 and 3), Floxed mice (Floxed/+; lane 4) and the null mice (−/−; lane 5). Southern analyses with 5′ internal probe 'a' and 3′ external probe 'b', drawn by striped bars, were carried out to detect the correct recombination in m*Lgr4* locus of ES cell clones and resultant mice.

of homology, and a 2.0-kb fragment spanning the end of exon 18 and the 3′-UTR was used as a 3′ arm of homology (fig. 3A). An intervening portion of exon 18 with flanking *lox*P sites (Floxed allele) was used to allow Cre recombinase-mediated deletion of part of this exon, deleting the LGR4 transmembrane domain and signal-transducing coding sequences (null allele; fig. 3A).

The targeting vector was linearized and electroporated into E14Tg2a ES cells as described previously [11, 13]. Approximately 400 G418 and FIAU-resistant colonies were screened by Southern blot analysis with an internal probe (shown as probe 'a' in fig. 3A). This probe recognizes 8.5- and 6.5-kb bands corresponding to the wild-type and targeted alleles, respectively. Confirmation of

the targeted clones was performed by Southern blot analysis with an external probe (shown as probe 'b' in fig. 3A) that recognized a 8.5-kb band wild-type allele, and 4.5-kb fragment corresponding to the Floxed allele (fig. 3B).

Four ES cell clones were found to be correctly targeted, corresponding to a targeting frequency of 1% in clones surviving selection. These were microinjected into C57BL/6 mouse blastocysts to generate chimeras. One chimera gave germline transmission, and was crossed with the CAG-Cre general deleter mouse [12] to remove the transmembrane coding sequence of the *Lgr4* gene and thus establish the heterozygous *Lgr4* mouse line. To confirm the deletion, tail DNA was prepared for genomic Southern blot analysis using the internal probe 'a'. We identified the newly generated 2.2-kb band corresponding to the null allele after excision exon 18 (fig. 3C).

Lethality in Lgr4 *Null Mice*

We genotyped pups at birth (P0) to estimate the ratio of wild-type and mutant *Lgr4* mice at birth (table 1B). Against the number of wild-type pups (n = 1,344), calculation with numbers from Mendelian expectation showed that 87.4% (n = 2,349) heterozygous and only 50.4% (n = 677) null pups were born. These data suggest embryonic loss of null mice.

Almost all of the newborn *Lgr4* null mice died within 2 days of birth (by day P2). Examination of their digestive organs revealed no evidence of suckling milk in contrast to their healthy littermates. One of the 2,105 pups surviving at weaning (P21) was a viable *Lgr4* null homozygous (table 1C); it showed severe growth retardation associated with death at P42 (see below).

To confirm the embryonic lethality of mutant mice, pregnant heterozygous females were sacrificed after timed mating with a heterozygous male for fetal genotyping between embryonic days E14.5 and E18.5. As shown in table 1A, the expected Mendelian frequency (wild-type:heterozygote:homozygote = 1:2:1) was maintained until E15.5; the numbers of heterozygous and null fetuses were measurably decreased after E16.5 and E18.5, respectively. Progressive loss of null mice continued throughout the E16.5–E18.5 interval. These data confirm the late embryonic lethality of the *Lgr4* null embryos. There were no statistical differences in lethality between sexes.

Gross Morphological Abnormalities of Lgr4 *Null Mice*

Tables 2 and 3 show body and organ weights among wild-type and mutant embryos aged E14.5–E19.5. There were no significant differences between the body weights of heterozygous $Lgr4^{+/-}$ and wild-type littermates over this interval. In contrast, *Lgr4* null mice showed a significant decrease in body weight on each embryonic day compared to heterozygous or wild-type siblings. The weight reduction of most organs in null animals reflected the proportional change in the order of whole body weight reduction (maintaining 70% of wild-type counterpart weights). However, among the organs analyzed, a more striking hypoplasia was noted in renal tissues, with the average kidneys contributing 0.51% overall to the total body weight in wild-type and $Lgr4^{+/-}$ mice, and 0.23% in the null mice (table 3).

Table 1. Number of embryos at each embryonic day, and of newborn and weaned pups

A Number of embryos on each day

	E14.5	E15.5	E16.5	E17.5	E18.5
+/+	36	31	38	30	33
+/–	68	65	73	55	50[a]
–/–	33	32	25[a]	21[a]	18[b]

B Number of pups at birth (P0, n = 4,370)

+/+ 1,344	+/– 2,349[a]	–/– 677[b]
Male 661	Male 1,187[a]	Male 330[b]
Female 683	Female 1,162[a]	Female 343[b]

C Number of pups at weaning (P21, n = 2,105)

+/+ 784	+/– 1,320[a]	–/– 1[b]
Male 382	Male 666[a]	Male 1[b]
Female 402	Female 654[a]	Female 0[b]

[a] $p < 0.05$, –/– vs. +/+. [b] $p < 0.01$, –/– vs. +/+.

Kidney Abnormalities in Lgr4 *Null Mice*

The normal kidney shows the highest expression on the *Lgr4* transcript (fig. 1), and renal weights were found to be severely reduced in *Lgr4* null mice. These findings indicate that the kidney would be the most severely affected organ in the absence of a functional *Lgr4* gene. Therefore, we focused our studies of $Lgr4^{-/-}$ mice on renal pathology.

Almost all of the *Lgr4* null mice died within 2 days of birth; one exception being a single mouse that survived to 6 weeks of age. The body weight of this survivor reached only 5.0 g at P28, while the weight of its littermates in-

Leucine-Rich Repeat-Containing G Protein-Coupled Receptor-4

Table 2. Overview of absolute embryonic body weights (g) in wild-type (+/+), heterozygous (+/–) and null (–/–) mice

	E14.5	E15.5	E16.5	E17.5	E18.5	E19.5
+/+	0.31 ± 0.02 (n = 24)	0.44 ± 0.02 (n = 25)	0.59 ± 0.02 (n = 26)	0.79 ± 0.02 (n = 23)	0.96 ± 0.01 (n = 27)	1.28 ± 0.01 (n = 21)
+/–	0.28 ± 0.01 (n = 48)	0.43 ± 0.01 (n = 44)	0.56 ± 0.01 (n = 41)	0.83 ± 0.02 (n = 52)	0.93 ± 0.02 (n = 45)	1.29 ± 0.02 (n = 39)
–/–	0.24 ± 0.02 (n = 21)	0.28 ± 0.02 (n = 23)[a]	0.46 ± 0.02 (n = 14)[a]	0.61 ± 0.02 (n = 14)[b]	0.79 ± 0.03 (n = 17)[b]	0.94 ± 0.03 (n = 13)[b]

Numbers tested are shown in parentheses with each data.
[a] $p < 0.05$, –/– vs. +/+ and +/–. [b] $p < 0.01$, –/– vs. +/+ and +/–.

Table 3. Overview of absolute organ weights and organ weight/body weight ratios in wild-type (+/+), heterozygous (+/–) and null (–/–) mice at birth (mean ± SEM)

Organ and units	Genotype		
	+/+	+/–	–/–
Body weight, g	1.55 ± 0.02 (n = 64)	1.54 ± 0.01 (n = 121)	1.08 ± 0.02 (n = 44)[a]
%	100	100	100
Liver, mg	54.64 ± 0.94 (n = 61)	54.87 ± 0.75 (n = 112)	35.54 ± 0.96 (n = 36)[a]
%	3.525 ± 0.02	3.563 ± 0.02	3.291 ± 0.03
Spleen, mg	3.64 ± 0.08 (n = 61)	3.69 ± 0.05 (n = 112)	2.58 ± 0.12 (n = 36)[a]
%	0.234 ± 0.02	0.240 ± 0.01	0.239 ± 0.02
Heart, mg	11.13 ± 0.19 (n = 61)	11.09 ± 0.14 (n = 112)	8.23 ± 0.25 (n = 36)[a]
%	0.718 ± 0.02	0.720 ± 0.01	0.762 ± 0.04
Lung, mg	41.63 ± 0.78 (n = 61)	40.75 ± 0.68 (n = 112)	31.20 ± 0.75 (n = 36)[a]
%	2.686 ± 0.02	2.646 ± 0.02	2.889 ± 0.05
Kidney, mg	7.99 ± 0.13 (n = 61)	7.81 ± 0.07 (n = 112)	2.43 ± 0.11 (n = 36)[a]
%	0.515 ± 0.02	0.507 ± 0.02	0.225 ± 0.07[a]
Testis, mg	0.88 ± 0.04 (n = 31)	0.83 ± 0.02 (n = 57)	0.69 ± 0.03 (n = 18)[b]
%	0.057 ± 0.01	0.054 ± 0.01	0.064 ± 0.01
Adrenal, mg	0.43 ± 0.01 (n = 47)	0.45 ± 0.01 (n = 79)	0.36 ± 0.01 (n = 28)[a]
%	0.028 ± 0.007	0.029 ± 0.007	0.033 ± 0.008

Organ weight/body weight ratios are given as percent. Numbers tested are shown in parentheses with each data.
[a] $p < 0.01$, –/– vs. +/+ and +/–. [b] $p < 0.05$, –/– vs. +/+ and +/–.

creased to approximately 15.0 g (fig. 4A). The kidneys of the null mouse were recovered just after it died and showed multiple fluid-filled cystic lesions (fig. 4B–D). On histological analysis, tubular epithelial cells appeared flattened, and vacuolar degeneration of these cells was pronounced. Proteinaceous debris can be seen inside the cystic lesions. The numbers of glomeruli were marked decreased. The remaining glomeruli did not show significant structural alteration by PAS stain, suggesting that their loss may be secondary to injury in the tubular nephron compartments. These findings are reminiscent of the histological hallmarks of human polycystic kidney disease and suggest a possible relationship between the *Lgr4* gene and this disorder (considered in the Discussion below).

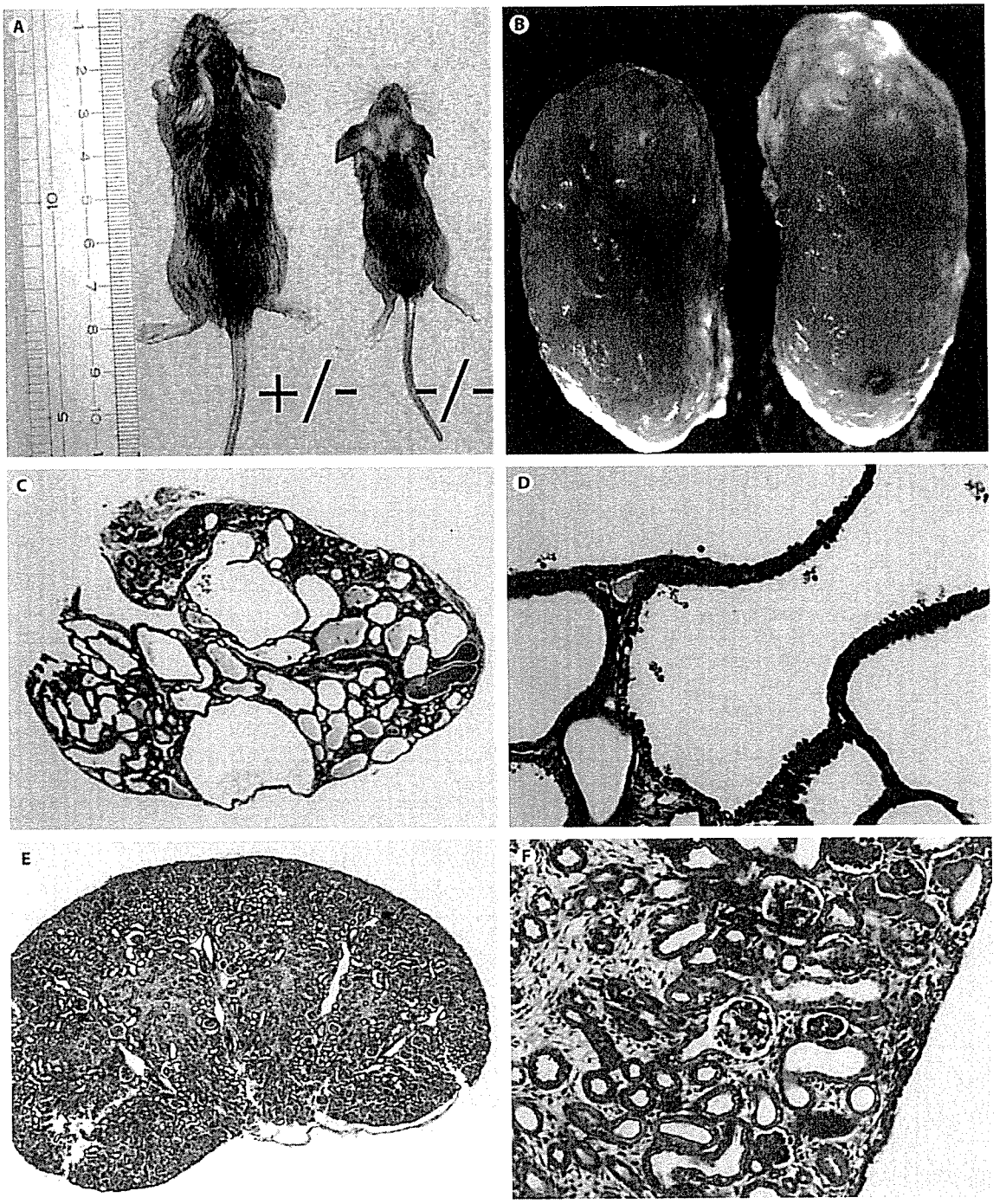

Fig. 4. Only one *Lgr4* null mouse of 667 littermates survived for 42 days. **A** Body length and appearance of a heterozygous mouse and its null littermate were compared at P28. **B** The kidney of the long-surviving null mouse is shown. The kidney was entirely swollen at the time of death with multiple cysts. Hematoxylin-eosin stains on kidney sections from P42 null and wild-type littermates. **C–F** Cysts are present in the kidneys of the null mouse (**C**, **D**), whereas the kidneys of a wild-type littermate mouse (**E**, **F**) appeared normal.

As illustrated in figure 5B, the sizes of kidneys of *Lgr4* null mice are significantly smaller than those of wild-type (and heterozygous; data not shown) littermates (fig. 5A), indicating renal hypoplasia. Spectrums of gross pathologies were appreciated in evaluating the gene-manipulated mice. Some showed hypoplastic kidneys with polycystic changes (fig. 5B, left kidney).

To assess renal function, plasma creatinine levels [14] were measured in *Lgr4* mutant and wild-type mice at birth (P0). As shown in figure 5C, a significant elevation in plasma creatinine levels can be observed in *Lgr4* null mice compared to wild-type mice at this early time point, demonstrating a lack of efficient clearance by the kidneys in *Lgr4* mutants. It is also important to note that the smaller $Lgr4^{-/-}$ animals have lesser muscle mass to contribute to a creatinine load, and so plasma creatinine levels alone, while instructive, likely underestimate compromises of their glomerular and tubular function.

Figure 6A–F show the histological findings of kidneys in wild-type and *Lgr4* null mice at birth (P0). Besides the overall size reduction (fig. 6B), kidneys from *Lgr4* null mice show significant reductions in glomerular and tubular numbers and density (fig. 6E, 7) compared to those of wild-type mice (fig. 6D, 7). In more than half of *Lgr4* null mice at birth, however, the basic structure of an individual glomerulus or tubule is maintained (fig. 6E). Some *Lgr4* null mice with high plasma creatinine levels at birth (P0) showed renal hypoplasia (fig. 6C) and absence of functional nephrons (fig. 6F). In several *Lgr4* null mice, more subtle asymmetries between the left and right kidneys (fig. 6G) were noted, with no differences in close histology (fig. 6H).

Given the reduced kidney sizes and elevated plasma creatinine concentrations seen, we suspected decreases in the number of functional nephrons in *Lgr4* null mice. Glomerular counting showed insufficient numbers of nephrons in these mice reflective of both kidney size and reduced glomerular density. Figure 7 indicates decreased total numbers of nephrons per unit area, suggesting that LGR4 contributes directly or indirectly to normal nephron density in the kidney (see Discussion).

To study any effects of *Lgr4* gene deficit on ureteric bud branching, the kidneys of E13.5 mice were histologically analyzed. Kidney samples from E13.5 wild-type (fig. 8A, C) and null (fig. 8B, D) embryos showed no obvious difference in their ureteric bud branching. In addition, a similar density of the ureteric bud tip was observed with both kidneys from wild-type and null mice (fig. 8E). These data imply that the *Lgr4* gene is more important to the development and maintenance of the glomerulus in

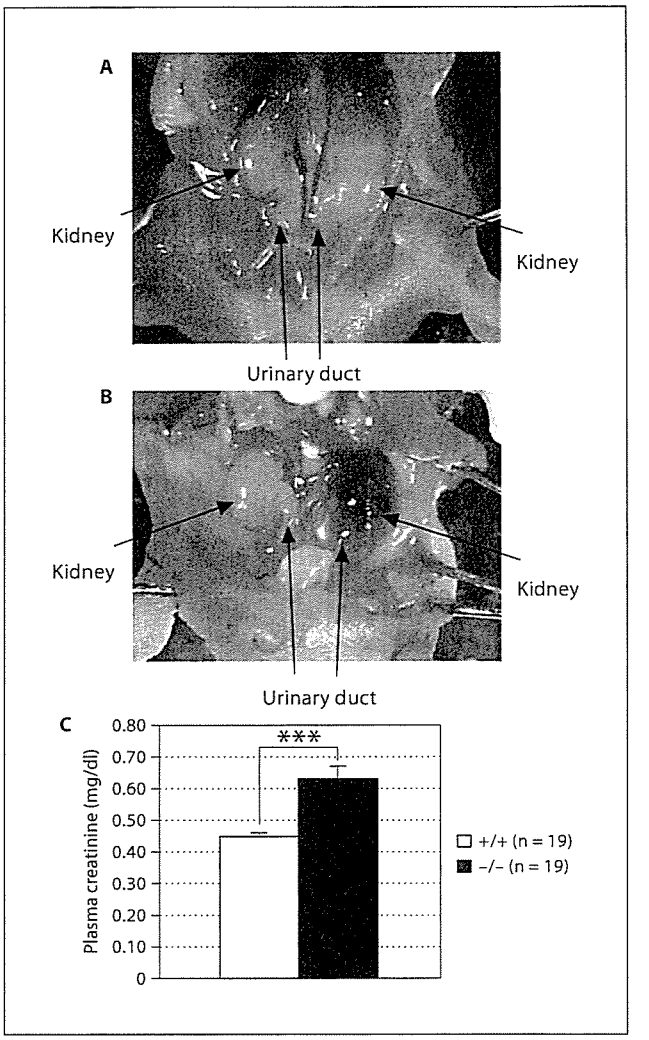

Fig. 5. Effects of *Lgr4* deficiency on the kidney of P0 mice. The morphology of the kidney and urinary duct in heterozygous (**A**) and null (**B**; no difference between wt and hetero mice; data not shown). The left kidney of the *Lgr4* null mouse shown was cystic. **C** To determine if the effects of *Lgr4* deficiency on the kidney were associated with functional changes, we measured plasma creatinine. *** $p < 0.001$, when compared with corresponding values from wt mice.

Fig. 6. Renal histopathology in the *Lgr4* null mice. Histology in a P0 wt mouse (**A**, **D**) and *Lgr4* null mice (**B**, **C**, **E–H**) is shown. Values on the left indicate the plasma creatinine concentration of each animal from which kidney and blood samples were prepared. **G**, **H** Unequally developed kidneys derived from a P0 null mouse. Each embedded kidney was sectioned at the region of maximum diameter. **A–C**, **G** Scale bar = 300 μm. **D–F**, **H** Scale bar = 60 μm.

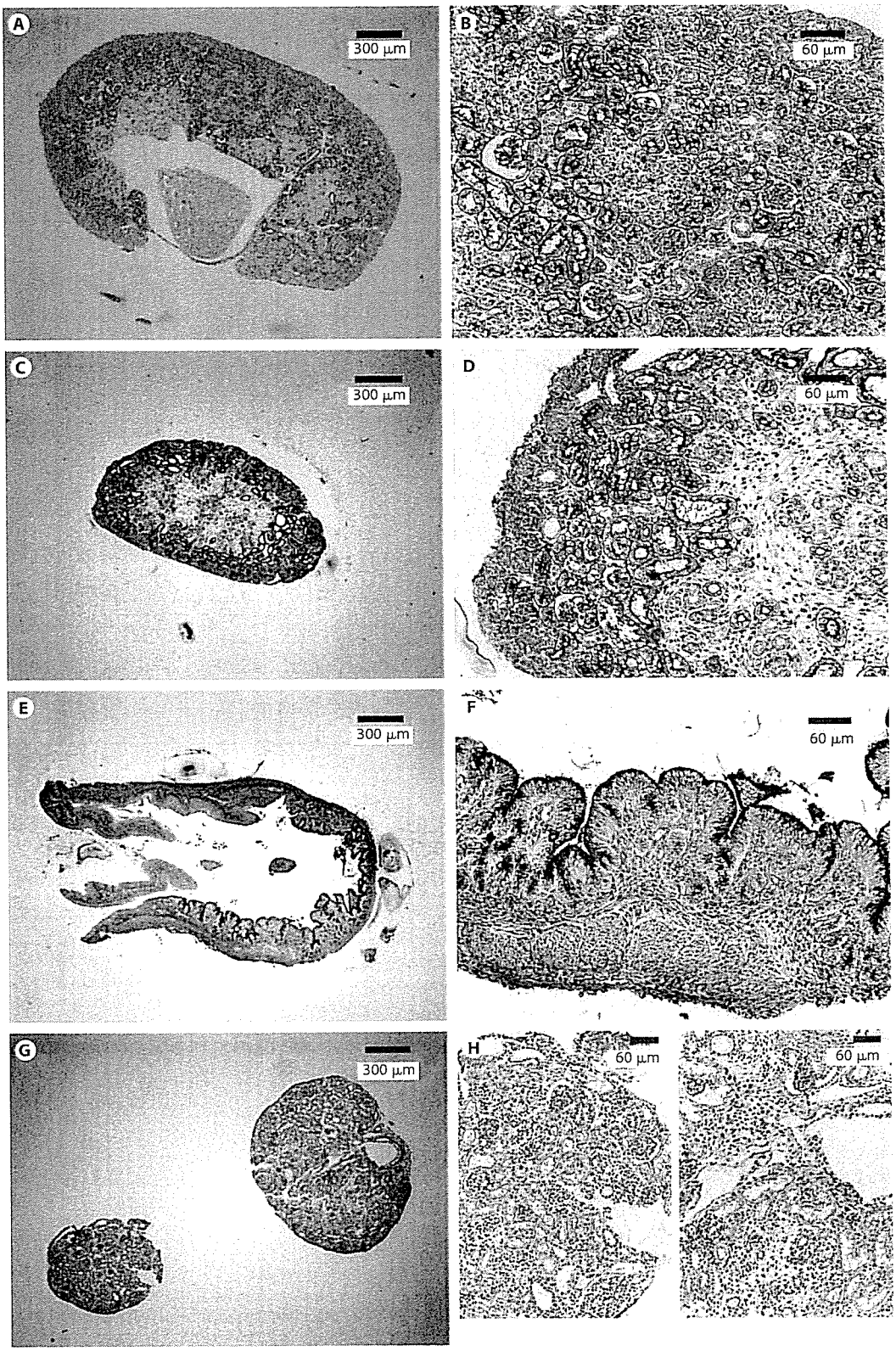
A
300 μm
B
60 μm
0.4
C
300 μm
D
60 μm
0.6
E
300 μm
F
60 μm
1.4
G
300 μm
H
60 μm
60 μm
0.8

6

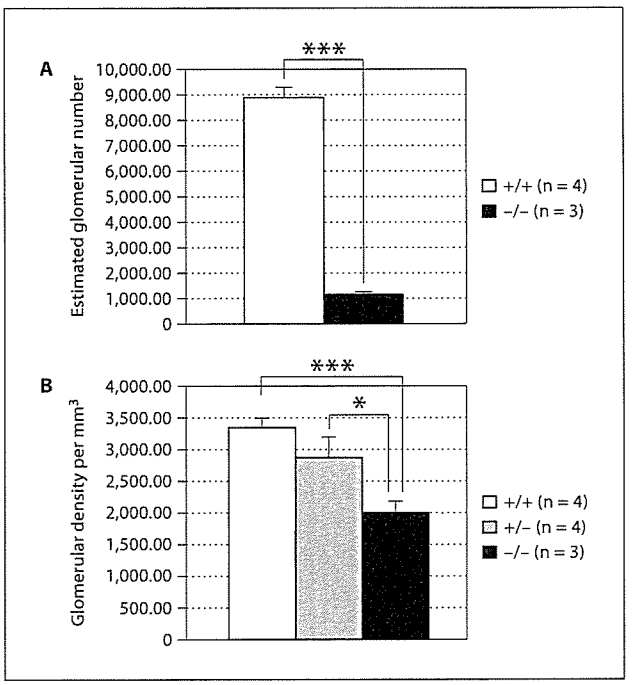

Fig. 7. Glomerular number (wild-type and *Lgr4* null) estimated and density (wt, *Lgr4* heterozygous and null) calculated in P0 mice. Mid slice sections were prepared, stained, and the numbers of glomeruli were counted. For an individual kidney, data from four non-adjacent sections (0.30 mm^2 apart; wt, heterozygous) or three non-adjacent sections (0.30 mm^2 apart; null) were obtained. Sections were prepared for 4 μm and wt kidney volume estimated 2.64 mm^3 and null estimated 0.58 mm^3. Data from 6 mice (wt and heterozygous) or 8 mice (null) were included. * $p < 0.05$ for null vs. heterozygous; *** $p < 0.001$ for null vs. wt.

later stages of kidney formation rather than to ureteric bud branching at early stages of nephron morphogenesis.

Discussion

In this report, we generated *Lgr4* gene-targeted mice with complete deletion of sequence encoding the LGR4 transmembrane and signal-transducing domains. Using the mutants, we demonstrate that *Lgr4* is required for normal kidney development and function to maintain filtration capacity without increasing the level of creatinine concentration. Null mice showed renal hypoplasia, and this phenotype was accompanied by functional failures as reflected in creatinine levels. Mazerbourg et al. [15] also recently reported the generation of a *Lgr4* knockout mouse model by gene trap methodology. They showed that deletion of *Lgr4* caused a phenotype most closely related to intrauterine growth retardation, to which they ascribed failure to thrive and perinatal lethality. However, abnormalities in individual organs possibly lead to perinatal lethality.

In contrast to the lower kidney weights in *Lgr4* gene trap mice seen by Mazerbourg et al. [15], the kidneys of null mice in our study are hypoplastic with a low density of glomeruli, leading to massive tissue damage in some cases, which indicates that *Lgr4* plays a critical role in kidney development. Despite kidney hypoplasia, however, a relatively normal glomerular structure was maintained until the accumulation of massive tissue damage. Although severe hypoplastic kidneys were observed in a few cases of *Lgr4* null mice, most of them showed merely a decreased kidney volume without structural defects. In contrast, 100% of *Lgr4* null mice showed an increased plasma creatinine concentration, perhaps reflecting an ensuing uremia contributing to perinatal death. Further experiments are required to discern whether the defect was simply caused by the decreased number of nephrons, or by a functional defect of the nephron unit in null mice.

Our findings suggest defects in the later stage of ureteric bud branching during nephrogenesis, although evagination of the ureteric bud and subsequent initial branching as well as differentiation of the metanephric mesenchyme have occurred normally in the null mice (fig. 8). Recent studies using knockout or transgenic mouse models have demonstrated the involvement of a number of key factors in determining nephron numbers, including fibroblast growth factor-10 [16, 17], *BMP-7* [18, 19] and so on. Although individual genes encoding these factors or receptors are expressed in various stages during nephrogenesis, they all share expression during branching morphogenesis. Kidneys of mice deficient in these genes showed histological phenotypes similar to the *Lgr4* null mice.

Although the ligand(s) and downstream effector(s) of LGR4 remain to be elucidated, the phenotype observed in the null mice allows us to speculate on the candidates. We expect that LGR4 will be involved with other molecules regulating the late stages of branching morphogenesis that determines nephron numbers. Mice with defects in GDNF-GFRα1-RET display renal hypoplasia [17, 20–22] similar to the LGR4 knockout phenotype. Profiling the gene expression in the null mice may also promote our understanding of the signaling pathway linked to

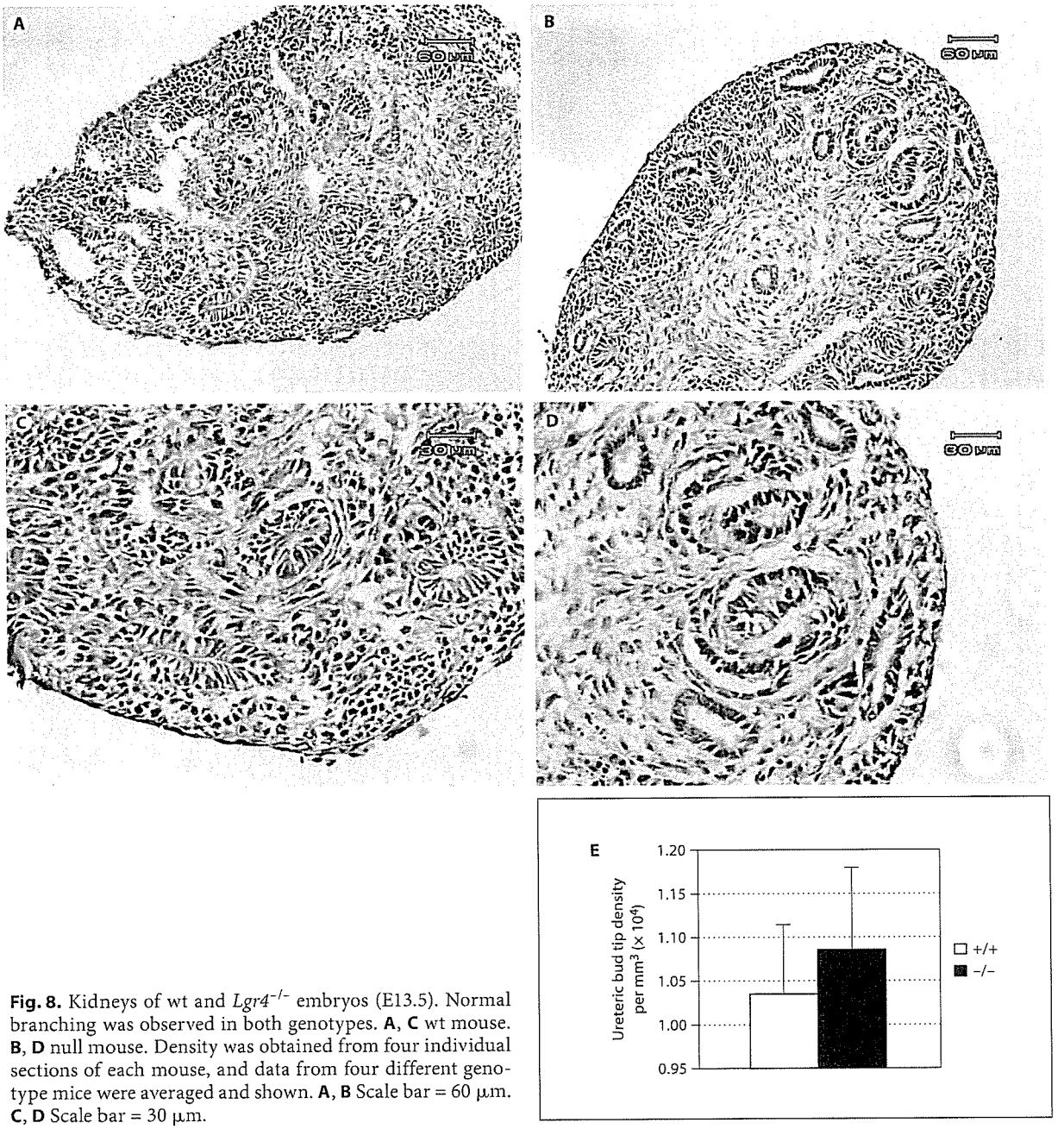

Fig. 8. Kidneys of wt and *Lgr4*$^{-/-}$ embryos (E13.5). Normal branching was observed in both genotypes. **A**, **C** wt mouse. **B**, **D** null mouse. Density was obtained from four individual sections of each mouse, and data from four different genotype mice were averaged and shown. **A**, **B** Scale bar = 60 µm. **C**, **D** Scale bar = 30 µm.

Lgr4. As some *Lgr4* null mice also display polycystic renal lesions, this suggests LGR4 might be involved in epithelial cellular polarity of other mechanisms that maintain renal tubule structure during nephrogenesis [23].

As compared to the study by Mazerbourg et al. [15], we observed greater penetrance of neonatal lethality and a more profound renal histopathological phenotype. The latter includes cystic lesions and a more subtle, perhaps precursor state of reduced nephron numbers and impaired renal function evident in mice surviving at birth (P0). These differences may be due to the different gene disruption strategies employed, or to genetic background

effects. Based on our findings we propose that renal dysfunction is a primary cause of the embryonic/neonatal lethality in *Lgr4* null mice.

In humans, the glomerular filtration rate is maintained in the face of renal insults, at first by the compensatory hyperfiltration of each glomerulus [24]. However beneficial in the short-term, prolongation of such overload causes glomerular sclerosis and renal failure in the long-term. Similarly, after uninephrectomy in young rats Nagata et al. [25] demonstrated that structural abnormalities in the glomeruli and a subsequent decrease in the glomerular filtration rate were never observed until 12 weeks after surgery. Some of the *Lgr4* null mice showed nephron agenesis with higher creatinine levels with first assessment at birth (P0; fig. 6C, F). In *Lgr4* null mice surviving to P2 and beyond, it is possible that gestational renal insults reach a critical state and manifest in renal failure early in postnatal life. Further experiments may be focused on assessing whether the severity of renal dysfunction in *Lgr4* null mice at birth and in the perinatal period is proportional to the extent of nephron number reduction as determined during nephrogenesis in utero.

While perinatal lethality was the predominant phenotype, one $Lgr4^{-/-}$ mouse survived longer. In histological analysis of its kidney upon necropsy, we observed dramatic cystic dilation of the renal tubules.

Other than the renal phenotype and intestinal dilation mentioned above, we also observed an the eyes open at birth phenotype in all of the *Lgr4* null mice. We have been studying the mechanism underlying this observation, and will report on this in the future.

In conclusion, we have generated a mouse model with complete deletion of *Lgr4* function and demonstrated that *Lgr4* is involved in nephrogenesis. We consider the lethality of *Lgr4* null mice as being closely related to renal dysfunction caused by impaired nephrogenesis. Circumventing the embryonic/neonatal lethal phenotype by a conditional knockout of *Lgr4* in mice will be useful for us to test this hypothesis and further study the functional role of *Lgr4* in individual tissues and organs.

Acknowledgments

We are grateful to Dr. T.R. Kumar (University of Kansas Medical Center) for his helpful discussions and critical review of the manuscript. We also thank Dr. N. Takamoto (Okayama University Medical School) for his valuable discussions and Dr. H. Suzuki for his encouragement. We thank Miss Y. Sato for providing the E14TG2a phage library. We also thank Dr. Y. Takayanagi for her excellent advice on manipulation of the mouse embryo. This work was supported in part by a grant-in-aid for scientific research (Hohga) from the Ministry of Education, Culture, Sports, Science and Technology of Japan (17659251) and by a grant from the Kureha Corporation.

References

▶1 Hsu SY, Liang SG, Hsueh AJ: Characterization of two LGR genes homologous to gonadotropin and thyrotropin receptors with extracellular leucine-rich repeats and a G protein-coupled, seven-transmembrane region. Mol Endocrinol 1998;12:1830–1845.

▶2 Heckert LL, Griswold MD: Expression of follicle-stimulating hormone receptor mRNA in rat testes and Sertoli cells. Mol Endocrinol 1991;5:670–677.

▶3 Sokka T, Hamalainen T, Huhtaniemi L: Functional LH receptor appears in the neonatal rat ovary after changes in the alternative splicing pattern of the LH receptor mRNA. Endocrinology 1992;130:1738–1740.

▶4 Hsu SY, Kudo M, Chen T, Nakabayashi K, Bhalla A, van der Spek PJ, van Duin M, Hsueh AJ: The three subfamilies of leucine-rich repeat-containing G protein-coupled receptors (LGR): identification of LGR6 and LGR7 and the signaling mechanism for LGR7. Mol Endocrinol 2000;14:1257–1271.

▶5 Krajnc-Franken MA, van Disseldorp AJ, Koenders JE, Mosselman S, van Duin M, Gossen JA: Impaired nipple development and parturition in LGR7 knockout mice. Mol Cell Biol 2004;24:687–696.

▶6 Kumagai J, Hsu SY, Matsumi H, Roh JS, Fu P, Wade JD, Bathgate RA, Hsueh AJ: INSL3/Leydig insulin-like peptide activates the LGR8 receptor important in testis descent. J Biol Chem 2002;277:31283–31286.

▶7 Kawamura K, Kumagai J, Sudo S, Chun SY, Pisarska M, Morita H, Toppari J, Fu P, Wade JD, Bathgate RA, Hsueh AJ: Paracrine regulation of mammalian oocyte maturation and male germ cell survival. Proc Natl Acad Sci USA 2004;101:7323–7328.

▶8 Hsu SY, Nakabayashi K, Nishi S, Kumagai J, Kudo M, Sherwood OD, Hsueh AJ: Activation of orphan receptors by the hormone relaxin. Science 2002;295:671–674.

▶9 Bullesbach EE, Schwabe C: LGR8 signal activation by the relaxin-like factor. J Biol Chem 2005;280:14586–14590.

▶10 Halls ML, Bathgate RA, Roche PJ, Summers RJ: Signaling pathways of the LGR7 and LGR8 receptors determined by reporter genes. Ann NY Acad Sci 2005;1041:292–295.

▶11 Matzuk MM, Finegold MJ, Su JG, Hsueh AJ, Bradley A: Alpha-inhibin is a tumour-suppressor gene with gonadal specificity in mice. Nature 1992;360:313–319.

▶12 Sakai K, Miyazaki J: A transgenic mouse line that retains Cre recombinase activity in mature oocytes irrespective of the cre transgene transmission. Biochem Biophys Res Commun 1997;237:318–324.

▶13 Nishimori K, Young LJ, Guo Q, Wang Z, Insel TR, Matzuk MM: Oxytocin is required for nursing but is not essential for parturition or reproductive behavior. Proc Natl Acad Sci USA 1996;93:11699–11704.

▶14 Duarte CG, Preuss HG: Assessment of renal function – glomerular and tubular. Clin Lab Med 1993;13:33–52.

▶15 Mazerbourg S, Bouley DM, Sudo S, Klein CA, Zhang JV, Kawamura K, Goodrich LV, Rayburn H, Tessier-Lavigne M, Hsueh AJ: Leucine-rich repeat-containing, G protein-coupled receptor 4 null mice exhibit intrauterine growth retardation associated with embryonic and perinatal lethality. Mol Endocrinol 2004;18:2241–2254.
▶16 Ohuchi H, Hori Y, Yamasaki M, Harada H, Sekine K, Kato S, Itoh N: FGF10 acts as a major ligand for FGF receptor 2 IIIb in mouse multi-organ development. Biochem Biophys Res Commun. 2000;277:643–649.
▶17 Qiao J, Bush KT, Steer DL, Stuart RO, Sakurai H, Wachsman W, Nigam SK: Multiple fibroblast growth factors support growth of the ureteric bud but have different effects on branching morphogenesis. Mech Dev 2001; 109:123–135.
▶18 Jena N, Martin-Seisdedos C, McCue P, Croce CM: BMP7 null mutation in mice: developmental defects in skeleton, kidney, and eye. Exp Cell Res 1997;230:28–37.
▶19 Dudley AT, Robertson EJ: Overlapping expression domains of bone morphogenetic protein family members potentially account for limited tissue defects in BMP7 deficient embryos. Dev Dyn 1997;208:349–362.
▶20 Sanchez MP, Silos-Santiago I, Frisen J, He B, Lira SA, Barbacid M: Renal agenesis and the absence of enteric neurons in mice lacking GDNF. Nature 1996;382:70–73.
▶21 Enomoto H, Araki T, Jackman A, Heuckeroth RO, Snider WD, Johnson EM Jr, Milbrandt J: GFR alpha1-deficient mice have deficits in the enteric nervous system and kidneys. Neuron 1998;21:317–324.
▶22 Jijiwa M, Fukuda T, Kawai K, Nakamura A, Kurokawa K, Murakumo Y, Ichihara M, Takahashi M: A targeting mutation of tyrosine 1062 in Ret causes a marked decrease of enteric neurons and renal hypoplasia. Mol Cell Biol 2004;24:8026–8036.
23 Wilson PD: Epithelial cell polarity and disease. Am J Physiol 1997;272:F434–F442.
24 Brenner BM, Garcia DL, S Anderson: Glomeruli and blood pressure. Less of one, more the other? Am J Hypertens 1998;1:335–347.
▶25 Nagata M, Scharer K, Kriz W: Glomerular damage after uninephrectomy in young rats. I. Hypertrophy and distortion of capillary architecture. Kidney Int 1992;42:136–147.